Atmos. Chem. Phys. Discuss., 11, 11143–11204, 2011
www.atmos-chem-phys-discuss.net/11/11143/2011/
doi:10.5194/acpd-11-11143-2011

Atmospheric Chemistry and Physics Discussions

Modelling of sea salt pollution over Europe: key uncertainties and comparison with observations

S. Tsyro[1], W. Aas[2], J. Soares[3], M. Sofiev[3], H. Berge[1], and G. Spindler[4]

[1]Norwegian Meteorological Institute, P.O. Box 43, Blindern, 0313, Oslo, Norway
[2]Norwegian Institute for Air Research, P.O. Box 100, 2027, Kjeller, Norway
[3]Finnish Meteorological Institute, P.O. Box 503, 00101, Helsinki, Finland
[4]Leibniz Institute for Tropospheric Research, Permoserstraße 15, 04318, Leipzig, Germany

Received: 4 March 2011 – Accepted: 23 March 2011 – Published: 11 April 2011

Correspondence to: S. Tsyro (svetlana.tsyro@met.no)

Published by Copernicus Publications on behalf of the European Geosciences Union.

Abstract

Sea spray can significantly affect the air quality. Sea salt can cause enhanced concentrations of particulate matter and change particle chemical composition, in particular in coastal areas, and therefore should be accounted for in air quality modelling. We have used an EMEP Unified model to calculate sea salt concentrations and depositions over Europe, focusing on studying the effects of uncertainties in sea salt production and lifetime on calculation results. Model calculations of sea salt have been compared with EMEP observations of sodium concentrations in air and precipitation for a four year period, from 2004 to 2007, including size (fine/coarse) resolved EMEP intensive measurements in 2006 and 2007. In the presented calculations, sodium air concentrations are between 8 and 46% overestimated, whereas concentrations in precipitation are systematically underestimated by 65–70% for years 2004–2007. Unfortunately, thus far performed tests have failed to give a clear answer regarding the reason for this underestimation and further studies are needed. The model is found to reproduce fairly well the spatial distribution of Na^+ in air and precipitation over Europe, and to capture most of sea salt episodes. The paper presents the main findings from a series of tests in which we compare several different sea spray source functions and also look at the effects of meteorological input and the efficiency of removal processes on calculated sea salt concentrations. Finally, sea salt calculations with the EMEP model have been compared with results from the SILAM model and observations for 2007. While the models produce fairly close results for Na^+ at most of 26 measurement sites, discrepancies in terms of bias and temporal correlation are also found. Those differences are probably due to differences in the representation of source function and treatment of sea salt aerosol, and also due to different meteorology used for model runs and due to a finer grid resolution of the SILAM model compared to EMEP. This study contributes to getting a better insight on uncertainties associated with sea salt calculations with the EMEP model and towards further improvement of EMEP aerosol modelling.

ACPD

11, 11143–11204, 2011

1 Introduction

Sea salt is a dominant aerosol type over oceans, also contributing significantly to the global aerosol burden. Sea salt aerosol plays an important role in atmospheric chemistry, providing the surface for heterogeneous reactions and acting as a sink for anthropogenic and natural gaseous tracers, e.g. for nitric and sulphuric acids. For example, the presence of sea salt aerosols in the atmosphere was shown to significantly alter the regional distribution of other inorganic aerosols, namely sulphate, nitrate and ammonium (van den Berg et al., 2000; Liu et al., 2006). Furthermore, sea salt is an important source of base cations which reduce the acidity of air and precipitation and increase soil base saturation. Thus, the deposition of base cations can partly counteract soil acidification and contribute to the recovery of ecosystems (van Loon et al., 2005).

With regard to air pollution issue, sea salt is a ubiquitous constituent of particulate matter (PM) and can significantly affect the air quality in coastal areas. Studies of the impact of sea spray on PM concentrations in coastal areas show that sea spray both enhances the levels and changes the chemical composition of PM (e.g. Pryor et al., 2007; Athanasopoulou et al., 2008). Sea salt contributes to the concentrations of PM_{10} and $PM_{2.5}$, which are chosen at present as air quality metrics, thus it has to be accounted for in air quality modelling in order to achieve a mass closure of PM and to provide accurate assessments of PM levels. In the European Commission's Air Quality directive (EC DIRECTIVE 2008/50/EC, 2008) it is stated that exceedences of PM can be corrected for natural contributions if these can be determined with sufficient certainty. Since measurements of sea salt contribution hardly can be determined for a larger spatial and temporal resolution, it is necessary with confidence in the model performance to conduct such corrections. Pryor et al. (2007) demonstrate that including sea spray in the model affects calculated composition and size distribution of PM and conclude that it is important to account for heterogeneous reactions on sea salt when evaluating the potential emission reduction measures to reduce PM in coastal cities. Model calculations in Athanasopoulou et al. (2008) also suggest enhanced nitrate formation

ACPD
11, 11143–11204, 2011

on sea salt particles over and downwind the shipping lanes in the Aegean Sea which, given the relatively low efficiency of deposition over sea, is transported to the land and contributes to PM pollution in Athens.

The generation of sea spray is commonly described with so-called source functions. Some of the proposed source functions are based on field measurements (e.g. Smith et al., 1993; O'Dowd et al., 1997; Andreas, 1998; Smith and Harrison, 1998; Vignati et al., 2001; De Leeuw et al., 2000), others on laboratory data (e.g. Monahan et al., 1986 and Mårtensson et al., 2003), or on both (e.g. Gong, 2003). In regional and global chemical transport models, the source functions by Mårtensson et al. (2003), Monahan et al. (1986) and Gong (2003) are broadly used to calculate bubble-mediated sea spray production and the schemes by Smith et al. (1993) and Smith and Harrison (1998) are used to calculate spume sea spray production. Comparative reviews of different source functions reveal that estimated sea spray fluxes vary by several orders of magnitude for different size ranges and wind speeds (Andreas, 1998; Guelle et al., 2001; Vignati et al., 2001; and Gong, 2003). Even source functions employing the same "white-cap method" differ by about a factor of 7 (Lewis and Schwartz, 2004). Given the uncertainties associated with calculating sea spray generation, an accurate reproduction of sea salt concentrations with chemical transport models is quite a challenging task.

In this work, we study the ability of the EMEP model to reproduce observed levels and the distribution of sea salt on a European scale for multiple years. First, we give a short overview of sea spray source functions and examine the behaviour of selected source functions using a box-model. Then, the sea salt parameterisation scheme presently implemented in the Unified EMEP model is described and calculation results are presented. The performance of the EMEP model for sea salt (i.e. sodium concentrations in air and in precipitation) is evaluated against observations for the years 2004–2007. A sensitivity analysis is performed to investigate the effect of modelling uncertainties on calculated sea salt concentrations as compared to measurements. We also compare sea salt concentrations calculated with the EMEP model employing different source functions and evaluate the model results against observations. Finally,

ACPD
11, 11143–11204, 2011

sea salt calculations with the EMEP model are compared with those from SILAM model of the Finnish Meteorological Institute. Compared to several earlier publications (e.g. Gong et al., 1997, 2002, 2003; Guelle et al., 2001; Grini et al., 2002; Foltesu et al., 2004), this work includes a comparative study of a larger number of sea spray source functions, presents multi-year sea salt calculations and the evaluation of model performance with a larger amount of observations, and it also provides a sensitivity analysis of calculated sea salt to the uncertainties in process formulations and input parameters.

2 Sea salt modelling

2.1 Sea spray source functions

Sea salt aerosols originate from sea spray droplets. The generation of sea spray occurs as the waves break on the surface of the ocean and whitecaps form causing the entrainment of air in the water. On the open ocean, this process is driven by the surface wind, whereas in the surface zone the wave breaking is largely due to their interaction with the sea bottom surface which intensifies the whitecap formation (de Leeuw et al., 2000). The size of sea salt aerosols strongly depends on the production mechanism. To avoid possible confusion concerning the size of sea spray droplets (Andreas et al., 2001), we will refer to their radii at a relative humidity of 80% (r_{80}) throughout this paper, unless different is specified.

Two main mechanisms responsible for sea spray formation are the air bubble bursting during whitecap formation and the direct tearing of droplets from the tops of breaking waves. The bubble-mediated mechanism produces two types of sea spray droplets. The first type is film droplets, which yield sea salt aerosol with radii between 0.25 and 2.5 µm. To produce film droplets, air bubbles larger than ca. 2.4 mm are required, each of which can give origin to between 100 and 1000 per droplets (Schulz et al., 2004). The second type of sea spray is jet droplets, with radii ranging between 1 µm and 8 µm (Guelle et al., 2001), or even reaching 25 µm (Andreas, 1998). The number of jet

ACPD
11, 11143–11204, 2011

droplets produced per a bubble decreases from 6 to 1 with increasing bubble size; and no jet droplets are produced from bubbles larger than 3.4 mm (Schulz et al., 2004). Spume droplets are formed through tearing of water right off the wave crests by wind. Spume sea spray forms aerosols which are typically larger than 10–20 µm, and wind speeds in excess of 10–12 m s^{-1} are needed for the generation of spume to take place.

A size dependent source function describes the number of droplets of a given size produced at the sea surface per unit surface area per unit time as a function of the surface forcing (i.e. wind speed, wave breaking, surface stress, etc). In this section, a short characterisation is given to some sea spray source functions, which are broadly used in regional and global transport models. Comprehensive overviews of sea spray functions can be found in Andreas (1998) and Schulz et al. (2004).

The source function of Monahan et al. (1986) for bubble-mediated sea spray combines data from shipboard photographic observations of whitecap formation with results from laboratory experiments, in which measurements were made of the size distribution of sea spray generated during the decay of a unit area of whitecap in a wave-tank. This scheme is valid for droplets with radii r_{80} between approximately 0.5 and 10 µm for 10-m wind speeds up to 9 m s^{-1}.

Smith et al. (1993) present the sea spray generation function constructed on the base of measurements taken in the Outer Hebrides (off the west coast of Scotland). The parameterisation was later modified by Smith and Harrison (1998) using sea spray measurements in the eastern North Atlantic. This source function is valid for sea salt particles between 1 and 150 µm for 14-m wind speeds in excess of 30 m s^{-1}.

Andreas (1998) constructed a combined sea spray generation function for droplets up to 250 µm. For droplets smaller than 10 µm, the parameterisation for bubble-mediated spray by Smith et al. (1993) is used, modified to fit the function by Monahan et al. (1986), whereas for spume spray the expressions are based on work by Andreas (1992).

ACPD
11, 11143–11204, 2011

Based on field measurements performed by O'Dowd et al. (1997), Vignati et al. (2001) developed an effective source function represented by a sum of three log-normal distributions. Fitting the calculations of size resolved sea salt flux with measurements from O'Dowd et al. (1997), Gong (2003) proposed modifications to the source function by Monahan et al. (1986) allowing its extension down to 0.080 µm of particle dry diameter.

Based on laboratory measurements, Mårtensson et al. (2003) derived a source function for production of sea salt aerosols with dry diameters between 0.02 and 2.8 µm. The proposed scheme calculates the production rate of size resolved sea salt aerosols as a function of the surface temperature for a water salinity of 33‰. In addition, sea spray concentrations were measured at several levels of water salinity, thus allowing the possibility of accounting for the dependence of sea salt generation on water salinity (Sofiev et al., 2011).

Clarke et al. (2006) used coastal field observations of sea salt number flux distribution combined with the assessment of near-surface concentrations due to observed bubble coverage from breaking waves to derive a source function for size resolved number flux.

Flux intensity and size distribution of sea spray depends on the concentrations and the spectrum of air bubbles, which can vary broadly due to a number of environmental factors (i.e. wind speed, sea water temperature and salinity, occurrence of organics films, wave breaking characteristics, atmospheric thermal stratification etc.). Therefore given the uncertainties associated with production conditions, it cannot be expected that a single universal sea spray source function can be formulated in terms of only few parameters (de Leeuw et al., 2003). Also Hoppel et al. (2002) cautions that all current formulations of source function are crude as they attempt to express the flux in terms of the current wind speed as the only variable. In reality, also other variables, such as a fetch, history of wind velocity, air-sea temperature difference, the thermal stability of the atmospheric and ocean surface layer, and surface-active material, play a role in sea spray generation.

ACPD
11, 11143–11204, 2011

A number of comparative studies conclude that the formulation of sea salt generation by Monahan et al. (1986) gives the soundest results for bubble-mediated sea spray. Guelle et al. (2001) found that for sea salt aerosols with dry diameters up to 4 µm, the source function by Monahan et al. (1986) provided the best match with observations. De Leeuw et al. (2000) reported that their source function for surf aerosol showed the best agreement with the open-ocean bubble-mediated source function of Monahan et al. (1986) for particle with dry diameters up to about 2.5 µm. Also Andreas (1998) concluded that the bubbles-only part of Monahan et al. (1986) spray generation function was at the moment the best available for predicting spray production by white cap bubbles. Further, Vignati et al. (2001) found an excellent agreement between the scheme from Monahan et al. (1986) and measurements of number size distribution of sea salt aerosols reported in O'Dowd et al. (1997) down to dry diameters of 0.4 µm. However, extrapolation of Monahan et al. (1986) source function to smaller sizes was shown to result in too great production of the number of smallest droplets (Vignati et al., 2001; Mårtensson et al., 2003). Also Gong (2003) concluded that Monahan et al. (1986) source function gave fairly good results for total sea salt mass and its wind dependence for sea salt aerosols larger than 0.4 µm dry diameter.

Pierce and Adams (2006) found that sea-salt mass concentrations from both Monahan et al. (1986) and Mårtensson et al. (2003) parameterisations were much lower compared to those from O'Dowd et al. (1997) and Clarke et al. (2006) functions. This is because the parameterisations by Monahan et al. (1986) and Mårtensson et al. (2003) predict lower emissions in super-micron sizes compared to O'Dowd et al. (1997) and Clarke et al. (2006), and there is no production of sea salt particles larger than 2.8 µm on Mårtensson et al. (2003) (see Fig. 2). Taking in to account the negative bias in wind speeds in their model, Pierce and Adams (2006) anticipated that model runs with O'Dowd et al. (1997) and Clarke et al. (2006) parameterisations were likely to overpredict the sea-salt concentrations in many locations. All in all, the authors found it difficult to say definitively which parameterisation was the best because of uncertainties in model meteorology, treatment of aerosol processing and in observational data.

ACPD
11, 11143–11204, 2011

Results presented in Ma et al. (2008) also indicate that Clarke et al. (2006) parameterisation tends to predict too large burden of sea salt.

Finally in several works, parameterisations of sea salt aerosol load over sea surface were derived, which were argued to be more directly connected to the observations compared to sea-spray fluxes. For example, Erickson and Duce (1988) described sea salt concentrations in surface air as a function of wind speed at 15m height. Lewis and Schwartz (2004) proposed a function for the average number size distribution of sea salt aerosols between 0.1 and 25 µm in diameter. Given the underlying assumption about equilibrium between the mean size distribution of sea salt aerosol and surface winds, this parameterisation may be considered better suitable for global models with rather coarse temporal and spatial resolutions, whereas it is not sound for much smaller time steps and grids (Ma et al., 2008).

2.2 Global and regional sea salt calculations

Evaluations of sea salt calculations with different models show rather variable results. Most of climate and global transport models compared calculated monthly averaged sea salt (Na^+) concentrations with observations (e.g. Gong et al., 1997b, 2002; Grini et al., 2002; Ma et al., 2008). Though most of model results were within a factor of two of observations on average, both significant over- and underestimations were reported for individual sites. For instance, Stier et al. (2005) found that calculated with ECHAM5 sea salt concentrations agreed within a factor of 2 with observations at remote marine sites, whereas they overestimated IMPROVE and GAW measurements by a factor of 2 to 10, especially for small concentrations. Using Monahan et al. (1986) within a global TM3 model, Guelle et al. (2001) found a fair agreement between calculated and measured monthly sea salt air concentrations (some underestimation in January–March for marine sites on Iceland and Ireland). For sea salt in precipitation, the model underestimated observations for most of the sites except the coastal ones, and by as much as an order of magnitude at sites away from the coast. Furthermore making use of Monahan et al. (1986) source function, FIZ-C climate model overestimated Na^+ in

ACPD
11, 11143–11204, 2011

air by 20–75% (Gong et al., 1997b), while GCMIII climate model underestimated Na^+ in air within a factor of 2 (Gong et al., 2002).

Using a combination of Monahan et al. (1986) and Mårtinsson et al. (2003) parameterisations, the regional model MATCH was found to severely overestimate Na^+ in air at Norwegian and Danish sites, whereas it underestimated only slightly for Dutch sites (Foltescu et al., 2004). Na^+ in precipitation was underestimated by about 40% by MATCH. Also the regional climate model RegCM, using a modified Monahan et al. (1986) function, overestimated sea salt in air by between 30 and as much as 300% (Zakey et al., 2008). Calculations from the regional climate/chemistry model REMOTE with sea salt parameterisation from Geever et al. (2005) produced Na^+ air concentration 2 to 6 times higher than observed (Langmann et al., 2008). Calculated Cl^- concentrations in precipitation were underestimated in January, while overestimated in June compared to measurements.

3 The EMEP model

3.1 General description

The full description of the EMEP chemical transport model is given in Simpson et al. (2003), Fagerli et al. (2004), Tsyro (2008), and can also be found on EMEP website http://www.emep.int. The model calculation domain covers the whole of Europe, and also includes a large part of the North Atlantic and Arctic areas. In vertical direction, the model is resolved with 20 layers, reaching a height of ca. 100 hPa. The lowest model layer is approximately 90 m thick. In the present calculations, the horizontal resolution of approximately $50 \times 50\,km^2$ was used. Meteorological model HIRLAM was used to drive most of presented simulations. Note that calculations prior the year 2007 were made using meteorological fields calculated with an older version of HIRLAM weather prediction model (called PARLAM-PS), while for 2007 an updated version of HIRLAM (version 7.1) was used. PARLAM-PS was run with $50 \times 50\ km^2$

ACPD
11, 11143–11204, 2011

resolution on a polar-stereographic projection, while HIRLAM was run on 0.2 × 0.2° rotated spherical grid and the meteorological field then were interpolated to the EMEP polar-stereographic projection. In addition to PARLAM-PS and HIRLAM v.7.1, meteorology from ECMWF-IFS (Integrated Forecast System) for 1996 was used in sensitivity tests. The ECMWF-IFS meteorological fields were retrieved on a geographical grid with 0.2 × 0.2° resolution. More in-depth study of the effect of using different meteorological drivers on EMEP model results, including verification of meteorological data, are documented in Tsyro et al. (2010).

The EMEP model describes the emissions, chemical transformations, transport and dry and wet removal of gaseous and aerosol components. The standard model version distinguishes two size fractions for aerosols, fine aerosol ($PM_{2.5}$) and coarse aerosol ($PM_{2.5-10}$). Dry deposition parameterisation for aerosols follows standard resistance-formulations, accounting for diffusion, impaction, interception, and sedimentation. Meteorology and land-use dependent dry deposition velocities are calculated for the two aerosol sizes, taking in to account particle hygroscopic growth. Wet scavenging is treated with simple scavenging ratios, accounting for in-cloud and sub-cloud processes. The scavenging ratios are assigned to crudely reflect the solubility of different aerosol components, and the size differentiated collection efficiencies are used in sub-cloud aerosol washout.

3.2 Parameterisation of sea salt production

The Unified EMEP model is primarily designed to calculate regional concentrations of $PM_{2.5}$ and PM_{10}. Hence standard model runs include sea salt particles with ambient diameters up to about 10 µm, which mainly originate from the bubble-mediated sea spray.

The parameterisation scheme for calculating sea salt generation in the EMEP model makes use of two source functions for bubble-mediated sea spray production. The first one is a source function from Monahan et al. (1986):

ACPD
11, 11143–11204, 2011

$$\frac{dF}{dr_{80}} = 1.373 \times U_{10}^{3.41} \times r_{80}^{-3}(1 + 0.057 r_{80}^{1.05}) \times 10^{1.19\ \exp(-B^2)} \quad (1)$$

where dF/dr_{80} is the rate of sea salt droplet generation per unit area of sea surface and per increment of droplet actual ("wet") radius, r_{80} is the aerosol radius at 80% relative humidity, U_{10} is the wind speed at 10 m, and $B = (0.380 - \log(r_{80}))/0.650$.

The second one is a source function from the work of Mårtensson et al. (2003), which is formulated for a salinity of 33‰:

$$\frac{dF}{d(\log d_d)} = 3.84 \times 10^{-6}(A_k T_w + B_k) \times U_{10}^{3.41} \quad (2)$$

where $dF/d(\log d_d)$ is the flux of sea salt aerosols per unit area of the whitecap cover and per increment of $(\log d_d)$, d_d is the dry diameter, T_w is the temperature of sea water, and A_k and B_k are the parameters describing the dependence of sea salt flux on the aerosol size:

$$A_k = C_4 d_d^4 + C_3 d_d^3 + C_2 d_d^2 + C_1 d_d + C_0$$

$$B_k = D_4 d_d^4 + D_3 d_d^3 + D_2 d_d^2 + D_1 d_d + D_0$$

The empirical coefficients C_i and D_i are tabulated according to Mårtensson et al. (2003).

In the EMEP model, the sea spray fluxes are calculated for particle dry diameters ranging from 0.02 to 10 µm, with a possibility to extend to larger sizes. The size range is divided onto size bins as shown in Table 1, and Mårtensson et al. (2003) parameterisation is applied for first six bins, while Monahan et al. (1986) parameterisation is used for the rest. Then, the total production rates of fine and coarse sea salt are found by integrating the size resolved fluxes over respective size intervals.

ACPD
11, 11143–11204, 2011

The relationship between the dry radius r_d and r_{80} of sea salt aerosols is expressed through an empirical formula of Gerber (1985), as suggested in Gong et al. (1997a):

$$r_w = \left[\frac{0.7674 r_d^{3.079}}{2.573 \times 10^{-11} r_d^{-1.424} - \log S} + r_d^3 \right]^{1/3} \quad (3)$$

The wind speed at the height $z_{10} = 10$ m is either taken directly from the NWP model, if available, or calculated within the EMEP model as

$$U_{10} = U_{ref} \frac{\ln\left(\frac{z_{10}}{z_0}\right) - \Psi\left(\frac{z_{10}}{L}\right) + \Psi\left(\frac{z_{10}}{L}\right)}{\ln\left(\frac{z_{ref}}{z_0}\right) - \Psi\left(\frac{z_{ref}}{L}\right) + \Psi\left(\frac{z_{ref}}{L}\right)} \quad (4)$$

In Eqs. (3) and (4), S is the saturation ratio, U_{ref} is the wind speed at the model lowest level z_{ref} (about 45 m), Ψ is the similarity function for momentum (Simpson et al., 2003). The roughness parameter z_0 is calculated using Charnock's relation (Stull, 1998; Garratt, 1992) as

$$z_0 = \beta \times u_*^2 / g \quad (5)$$

where u_* is the friction velocity, g is the gravitational acceleration, and β is the empirical constant. In the present version of the EMEP model $\beta = 0.0114$ is adopted.

In the model, generated sea salt aerosols are assumed to be instantaneously mixed within the model lowest layer (approximately 90 m height) at each time step. Then, the transport and removal of sea salt is described individually for the fine and coarse fractions in the EMEP model.

4 Measurements

Measurement data used in this work are primarily the concentrations of sodium (Na^+) in air and precipitation in the years from 2004 to 2007 from EMEP monitoring network.

ACPD
11, 11143–11204, 2011

The list of stations and their details are provided in Table A1 in the Appendix. In addition, data obtained during two EMEP intensive measurement periods in June 2006 and January 2007 have been used.

In the regular EMEP measurements of sodium air concentrations, aerosols are commonly sampled using a filter pack sampler (EMEP, 1995) with a daily sampling frequency. This sampler has no defined cut off, but it normally captures particles about PM_{10} size depending on the flow rate. Teflon aerosol filters are usually employed and the analytical method for sample analysis is mainly ion chromatography. Precipitation is commonly sampled using a wet only sampler, which is the recommended method in EMEP. However there are a few countries using bulk collectors. Details of sampling and analytical methods can be found in Hjellbrekke and Fjæraa (2009). The quality of the analytical performance is checked annually in the EMEP lab inter-comparison (e.g. Uggerud, 2009) and the standard deviation is generally around 5%. In the intensive measurements periods the methodology was different. There were PM_{10} and $PM_{2.5}$ (and PM_1) samplers, usually low volume sampler with a quartz filter.

The predominant source of sodium is ocean and sea water, though there are some anthropogenic sources that may contribute to sodium concentrations to some extent. For instance, Maykut et al. (2003) identified craft pulp mills as a possible source of sodium in Seattle. Furthermore, salting of icy roads may be an important source in areas with winter climate, but a study by Blomqvist and Johansson (1999) showed for Stockholm that ninety per cent of the total deposition occurs within 20 m from the road.

The size distribution of sea salt in marine air shows only one peak in the coarse particle range (Sellegri et al., 2001), whereas it may have different size distribution in inland air. A study by Ookii et al. (2002) in Japan showed bimodal peaks in the fine and coarse particle range. They stated that in urban areas in Japan incineration plants account for a large fraction of the total sodium emission, and the average concentration of fine sodium in urban air was three times higher than that in marine air. In Europe, anthropogenic emissions of sodium is reported from various combustion and industrial processes, highest percentage contribution is from glass production (Hellsten et al,

ACPD
11, 11143–11204, 2011

2007). Combustion of lignite for domestic heating is one of the main anthropogenic sources of sodium in Germany (G. Spindler, personal communication, 2010). Van Loon et al. (2005) estimated that anthropogenic emission of sodium contributes with 1.1% of the coarse primary PM, 0.7% of the fine PM.

The Na/Cl mass relationship of 0.56 as in sea water (Millero, 2004; Warren, 2009) could be an indicator whether the salt is mainly from sea salt, though anthropogenic sodium that is emitted as NaCl is often difficult to distinguish from sea-salt NaCl. Furthermore, chloride depletion occur because of evaporation of HCl altering the Na/Cl ratio (Warren, 2009), this is especially an issue for aged sulphuric acid containing particles.

5 Results from sea salt calculations

5.1 Comparative study within box-model

In this section, we compare sea spray fluxes calculated with a box-model using different source functions. Learning about the difference between source functions with respect to the size distribution of sea spray and to its dependence on wind speed will facilitate our interpretation of results for sea salt calculated with the EMEP model.

We mainly focus on the source functions which cover generation of sea spray sizes down sub-micron and ultra-fine region, i.e. combined Mårtensson et al. (2003) and Monahan et al. (1986), Vignati et al. (2001), Gong (2003) and Clarke et al. (2006), which will be referred to as M&M, V01, G03 and C06 respectively. Parameterisations by Andreas (1998) and Smith and Harrison (1998) (A98 and SH98) are only valid for sea spray droplets with wet diameters exceeding 2 µm, however A98 is also shown here. We investigate the differences in the size distribution of generated sea salt particles and the dependence of sea salt fluxes on the wind speed. The comparison is limited to bubble-mediated sea spray droplets with radii r_{80} up to about 10 µm. The

ACPD
11, 11143–11204, 2011

same discretisation of the spray size range has been applied in calculations with all considered source functions.

Figure 1 shows the number and volume fluxes of sea spray for 10 m wind speed of 10 m s^{-1} calculated with M&M, G03, V01 and A98 source functions. The fluxes are plotted as a function of the droplet size (r_{80}). The source function by Mårtensson et al. (2003) includes the dependence of sea salt generation on the temperature of sea water. Sea salt fluxes calculated with M&M for the sea temperature of 10°C and 20°C are shown in Fig. 1.

M&M number and volume fluxes of spray are larger than those from G03 and V01 for droplets smaller than about 2 µm. Results for M&M with different temperature of sea water show that for the same wind speed, warmer sea water (20°C) produces fewer droplets that are smaller than 0.1 µm, but more droplets that are larger than about 0.2 µm compared to the colder water (10°C). As pointed out above, A98 parameterisation is limited to sea spray droplets with r_{80} larger than 1 µm. Thus, A98 fluxes differ significantly from the other source functions, with A98 greatly underestimating fluxes of the smallest droplets.

Figure 2 shows the size dependence of sea spray fluxes calculated with M&M, G03, V01, C06 and A98 source functions for wind speeds of 5, 10 and 15 m s^{-1} (note that the results are presented in two graphs in order to avoid having an over-complex figure). Shown are the fluxes of sea spray number (left picture) and volume (right picture). Figure 2 reveals that the sea spray fluxes calculated with the different source functions exhibit different dependencies on the wind speed both with respect to the intensity and the size distribution of sea spray droplets.

In summary, the comparison study between the selected source functions has shown that:

– The largest discrepancies in sea spray fluxes (up to two orders of magnitude) are found for droplets with r_{80} smaller than 0.1 µm. Based on O'Dowd (1997) field measurements, V01 and G03 both predict a flux peak around 0.2 µm, while in the parameterisation by Mårtinsson et al. (2003) the sea salt flux peaks at around

ACPD
11, 11143–11204, 2011

0.07 µm. Sea spray fluxes of this size range contribute greatly to the sea salt particle number, but negligibly to the mass;

- M&M and G03 fluxes are quite close for all wind speeds for sea spray larger than about 0.4 µm. This is not too surprising since G03 was derived based on Monahan et al. (1986) formula;
- stronger wind dependence of sea spray fluxes is apparent for G03 and M&M source functions compared to V01. Particularly pronounce differences are found for lower winds (e.g. 5 m s^{-1}), for which V01 calculated sea spray fluxes are much larger than those from M&M and G03 schemes;
- C06 shows wind dependence of sea spray flux similar to that from M&M, while the size distribution of sea spray droplets from those schemes are different, namely C06 calculates smaller fluxes of sea salt aerosols below r_{80} of 0.2 µm, but larger fluxes for larger droplets as compared to M&M.

5.2 Calculations with the EMEP model

The combined source function M&M based on Mårtensson et al. (2003) and Monahan et al. (1986) is used to calculate sea salt aerosol production within the Unified EMEP model, version rv3.1 (Simpson et al., 2003; Tsyro, 2008). Results of comparison of model calculated sea salt concentrations with observations are documented in EMEP reports (e.g. EMEP Reports 4/2006, 4/2007, 4/2008 and 4/2009 at http://www.emep.int).

In this paper, we present results from EMEP model calculations of sea salt aerosol and comparison with observations for the years from 2004 to 2007. For 2006, we compare sea salt results from the standard EMEP model with those using source functions G03, V01 and A98 within the EMEP model.

Annual mean concentrations of sea salt for the year 2006 calculated with the EMEP model using different source function are presented in Fig. 3. Sea salt particles up

ACPD
11, 11143–11204, 2011

to approximately 10 µm in diameter at the ambient relative conditions are accounted for. The largest sea salt concentrations are produced by C06 source function, which is consistent with results of calculations in Pierce and Adams (2006) and Ma et al. (2008). Somewhat lower sea salt levels are calculated using V01, while the lowest sea salt concentrations come from SH98 parameterisation. The sea salt concentrations from G03 are quite close to the EMEP standard results, whereas sea salt concentrations from A98 are somewhat lower.

Figure 4 displays two vertical cross-sections of sea salt for geographical locations shown in the small maps. The enhanced sea salt concentrations associated with emission areas are pronounced up to about 600–700 m. The concentrations drop by about an order of magnitude at 1 km height, where sea salt is still present at concentration levels of 1–2 $\mu g\,m^{-3}$. At 2–3 km heights, sea salt concentrations are about two orders of magnitude smaller than in the surface layer. Further up, sea salt is present at very low concentrations and shows quite uniform horizontal distribution.

6 Comparison with measurements

The performance of the EMEP model for sea salt has been evaluated through comparison with data from the EMEP monitoring network and from the EMEP intensive measurements. Measurements of sodium (Na^+) concentrations described in Sect. 4 have been used for this purpose. From model calculations, Na^+ concentrations have been derived as 34% of sea salt mass. In this section, results for standard model calculations, i.e. using M&M parameterisation, are shown, while results for calculations using the other parameterisations are presented in the following section.

6.1 Comparison with EMEP monitoring data

Table 2 summarises the results of annual statistical analysis of model calculated versus measured Na^+ concentrations in air and precipitation for the years from 2004 to 2007.

ACPD
11, 11143–11204, 2011

The model overestimates the measured Na^+ air concentrations in all years, but the underestimation decreases from 46% in 2004 to 8% in 2007. One of the reasons for the decrease of model's positive bias is a gradual increase of the number of stations with Na^+ measurements in central Europe between 2004 and 2007, for which the model shows a tendency to underestimate Na^+. In addition, changes in model results for 2007 are also due to the use of a new meteorological driver, namely an updated version of the HIRLAM model. It was shown in Tsyro et al. (2010) that due to a more intensive upward turbulence dispersion and more precipitation in HIRLAM meteorology, the EMEP model calculates surface concentrations of all aerosols somewhat lower compared to when using PARLAM-PS meteorology.

If only the sites are considered where Na^+ air concentrations were measured in all of the years from 2004 to 2007, the model bias varies from 36% in 2004 to 26% in 2005 and to 35% in 2006. Again, it decreases to 15% in 2007 partly due to changing the meteorological model. The fairly good correlation between calculated and observed annual mean Na^+ concentrations indicates that the model realistically describes the geographical distribution of sea salt over Europe. For Na^+ in air, the spatial correlation coefficients lie between 0.76 and 0.81, while for Na^+ in precipitation they are between 0.70 and 0.93 in the considered period.

Measurements of Na^+ concentrations in precipitation are available at a larger number of EMEP stations compared to air concentration monitoring, in particular at more in-land sites. Contrary to Na^+ air concentrations, the model underestimates Na^+ concentrations in precipitation by between 63 and 73% for the years 2004–2007. At the same time, the calculated precipitation is only slightly biased and thus cannot explain the model underestimation of Na^+ in precipitation. The model underestimates Na^+ in precipitation at all sites, regardless whether Na^+ in air is over- or underestimated, and no clear correspondence has been found in model performance for Na^+ in air and in precipitation between the sites. Also, the model underestimation of Na^+ in precipitation is about the same order of magnitude both at coastal and in-land sites. If we only look at the sites with concurrent measurements of Na^+ in air and in precipitation,

ACPD
11, 11143–11204, 2011

which are mainly coast sites, the model calculations are positively biased (by between 28 and 71%) for Na^+ in air, while results for Na^+ in precipitation are negatively biased (between −55 and −74%) compared to observations. As seen in Table 2, annual accumulated wet deposition of Na^+ is underestimated by between 69 and 77% in the period 2004–2007.

Seasonal analysis shows that the model reproduces well the average seasonal variation of sea salt for the period 2004–2007, characterised with minimum in summer and maximum in winter (Table 3). The model overestimates observed Na^+ concentrations by about 25% in all seasons, and less so (by 13%) in the summer period. Model underestimation Na^+ in precipitation is somewhat smaller in summer compared to the other seasons. Available verifications of precipitation input data cannot explain discrepancies between calculated and observed Na^+ in precipitation and Na^+ wet deposition, as the accumulated precipitation rather tends to be slightly overestimated.

For individual EMEP sites, the average model bias is 23% and the average temporal correlation with measurements is 0.56 for the years 2004–2007, though both vary considerably between the sites (Table A2). Calculated values of Na^+ air concentrations lie within 30% and 50% of measured values at 78% and 93% of the sites respectively. Figure 5 shows the annual mean model bias and correlation at the EMEP sites ranked from left to right according to increasing observed Na^+ concentrations for 2006. At the sites distant from the sea, mean Na^+ concentrations are typically below 0.5 $\mu g\,m^{-3}$, with the lowest Na^+ levels being measured at the most far-off from the coast locations. For in-land sites, the model bias is in general larger and can be both positive and negative, but the greatest underestimations are found for the most remote from the sea sites (SK04, SI08, DE03, AT02). It should be noted that at in-land sites also anthropogenic sources can contribute to sodium concentrations, whereas none of anthropogenic sources have been accounted for in the model. At the sites experiencing more or less direct influence from the sea Na^+ concentrations are in a range of 0.6 to 3.7 $\mu g\,m^{-3}$. Calculated Na^+ in air agrees with observations at the sites located closer to coasts better than for in-land sites, with the model showing a slight tendency to

ACPD
11, 11143–11204, 2011

overestimation (though Na^+ is quite underestimated at IE08). The temporal correlation between calculated and measured Na^+ in air is rather poor at the most remote from the sea sites (AT02 and SK04), as accurate calculation of day-to-day variability of very low concentrations are indeed a difficult task. The correlation significantly improves with decreasing distance to the coast, but goes slightly down at coastal sites (IE01, IE06 and IE08). The latter could probably be explained by the non-representativeness of measurements at coastal stations for a grid cell of 50×50 km^2 used in the model calculations.

6.1.1 Comparison with EMEP intensive measurements

During EMEP intensive measurement periods in June 2006 and January 2007, measurements of Na^+ in both PM_{10} and $PM_{2.5}$were performed at a number of sites. These measurements for the first time facilitated evaluation of model calculated size distribution of sea salt between fine and coarse aerosols in summer and winter seasons. For comparison with model calculations in this work, we have selected only those sites, at which the data coverage was at least 75% of days during each of the measurement months. The selected sites are Birkenes (NO01), Virolahti (FI17), Montelibretti (IT01) and Melpitz (DE44) (the only exception is FI17, for which only 12 days with Na_$PM_{2.5}$ data were available for June 2006).

Average values of observed (Obs) and modelled (Mod) air concentrations of Na^+ in PM_{10} and $PM_{2.5}$ for the intensive measurement periods are provided in Table 4. Both model and observations show higher Na^+ air concentrations in January 2007 compared to June 2006, which is due to typically higher wind speeds in winter. The correlation (R) between calculated and measured Na^+ show considerable variation between the sides and the months, ranging from −0.25 to 0.88. The correlation is mostly better than 0.40 for NO01, FI17 and DE44, but it is poorer for IT01.

Figure 6 summarises the statistical analysis with respect to model's bias compared to observations at those four sites. Shown are the results for concentrations of Na^+ in PM_{10} (Na_PM_{10}) and separately for fine (Na_$PM_{2.5}$) and coarse Na^+ in June 2006 (left)

ACPD
11, 11143–11204, 2011

and January 2007 (right). It should be noted that concentrations of coarse Na^+ was not measured, but have been derived as the difference between measured Na_PM_{10} and Na_$PM_{2.5}$. This means that they can be affected by uncertainties in measurements of both Na^+ in PM_{10} and $PM_{2.5}$ and thus, should be considered with caution. Also, note that fewer days with measurements were available for Na^+ in $PM_{2.5}$ (and thus for coarse Na^+) than for Na^+ in PM_{10} at FI17, causing some inconsistency in the analysis.

Na^+ air concentrations in both fine and coarse fractions are underestimated by the model in the summer month of June 2006 (with the exception of Na^+ in PM_{10} at FI17). The underestimation of Na^+ concentrations is smaller (within 40%) at NO01 and FI17 which are situated closer to the sea compared to IT01 and DE44, at which Na^+ is underestimated by between 40 and 70% for June 2006. In the winter month of January 2007, the model tends to overestimate Na^+ concentrations at FI17 and NO01, at the same time the underestimation of Na^+ is considerably smaller than in summer in both size fractions at IT01 and DE44. Furthermore compared to observations, the model tends to attribute a larger portion of PM_{10} Na^+ to the fine mode in June 2006, while it puts somewhat too much Na^+ in the coarse mode in January 2007 (not shown here).

We look closer at the distribution of Na^+ between fine and coarse particles for DE44 (Melpitz), for which Na^+ measurements in PM_{10} and $PM_{2.5}$ are available for the whole year of 2007. The daily time-series of Na^+ in PM_{10},$PM_{2.5}$ and coarse Na^+ (found as the difference of those) are shown in Fig. 7. The model quite closely reproduces observed Na^+ concentrations, somewhat underestimating Na^+ in all of the size fractions. Na^+ distribution between the two size fractions is fairly well calculated. Also, the model describes well the seasonal variation of Na^+, however showing a tendency to underestimate Na^+ somewhat more in warm period. Day-to-day Na^+ variation, including Na^+ pollution episodes, is also well calculated by the model.

In summary, the comparison of model results for Na^+ air concentrations with EMEP intensive measurements at four sites indicates that calculated production of sea salt mass is probably somewhat too small in summer, but is more accurate in winter. The

ACPD
11, 11143–11204, 2011

reason for that could be too low wind speeds in summer as calculated by the meteorological model or inaccurate description of the wind speed dependence of sea spray flux. On the other hand, the resolution of the EMEP of 50 × 50 km^2 could be too coarse to accurately reproduce sea salt gradients.

The results also indicate a possibility of too efficient removal of sea salt aerosol from the air, as Na^+ air concentrations tend to be larger under-predicted by the model at the sites farther from the sea.

All in all, the model calculated distribution of sea salt mass between fine and coarse aerosols is quite close to the observed one, namely the fraction of fine Na^+ mass within Na^+ in PM_{10} are on average 0.36 from the model and 0.4 from the measurements. Still, some seasonal discrepancies are found between calculations and observations for some individual sites, for which model results suggest that in summer more Na^+ resides in fine fraction compared to winter, which is not seen in the measurement data. This implies that the wind speed dependence of the size distribution of sea spray flux calculated with M&M parameterisation needs further testing and evaluation.

7 Uncertainty study

The performance of the model for sea salt strongly relies on the precision of calculations of sea spray production and sea salt size distribution at different ambient conditions. However, beside the accuracy of the sea spray source function, the ability of the model to reproduce sea salt concentrations greatly depends on the quality of wind speed data used in model calculations. Also, an accurate description of processes related to sea salt transport, dry and wet deposition is essential. For example Pierce and Adams (2006) demonstrated the importance of model processes other that sea salt emissions parameterisation and cautioned against concluding that the emissions parameterisation is superior to other processes and parameters when explaining the model results.

ACPD
11, 11143–11204, 2011

A series of test runs has been carried out in order to study the effect of uncertainties in sea salt generation and removal efficiency on model results, trying to reconcile them with observations. In this section, we compare model sea salt results using different source functions. We also investigate the effect of dry deposition and wet scavenging velocities on calculated sea salt.

7.1 Effect of sea spray source function

As shown in Fig. 3, differences in calculated sea salt fields can be quite large when using different sea spray source functions. In this section, we compare results from the standard EMEP model run using four alternative parameterisations of sea salt production with observations for 2006. Tables 5 and 6 summarise the comparison statistics for Na^+ concentrations calculated using source functions M&M, G03, A98, SH98 and V01 (see for explanation Sect. 2.1 and 5.1). The statistics are shown for the whole year of 2006 and for four seasons.

The main findings from Tables 5 and 6 are:

- M&M and G03 parameterisations give quite similar results for Na^+ air concentrations. They overestimate the annual mean Na^+ by 12 and 25% respectively in 2006;

- A98 and SH98 underestimate Na^+ air concentrations by 10 and 40% respectively. Lower concentrations of sea salt from A98 is partly due to its underestimation of sea spray production for droplets under 2 µm compared to M&M and G03 (see Fig. 1). On the other hand, A98 produces more sea salt mass on larger particles, especially at lower wind speeds. Using A98 source function, Guelle et al. (2001) got a general overestimation of sea salt concentrations at eight stations around the globe and attributed that to a very efficient sea salt production at low wind speeds. However in this work, calculations with the EMEP model using A98 source function do not overestimate observations. The reason for that could be

ACPD
11, 11143–11204, 2011

that the largest sea salt particles are removed more efficiently by gravitational settling in our calculations;

- V01 parameterisation gives far too high sea salt concentrations, overestimating the Na^+ observations by 120%;
- for different seasons, the best agreement with observations for M&M and G03 predictions of Na^+ air concentrations is found in summer-autumn, when positive bias decreases. On the contrary, Na^+ concentrations calculated with A98 are closer to the observations in winter-spring (a light negative bias), while they overestimate observations by 26–27% in summer-autumn. Those differences in seasonal predictions are probably because compared to M&M and G03, A98 calculates larger sea salt productions at low wind speeds which are more typical for summer-autumn months. SH98 considerably underestimates Na^+ air concentrations in all seasons, though somewhat less in winter, while V01 is found to significantly overestimate Na^+;
- the spatial correlation between annual mean calculated and measured Na^+ concentrations is quite similar for all parameterisations, with the correlation coefficient ranging between 0.76 for SH98 and 0.79 for M&M. The spatio-temporal correlation (between calculated and measured daily Na^+ concentrations for all sites) and the correlation for the individual seasons is the best for M&M source function, closely followed by G03 and SH98, and considerably lower correlation is found for A98 and V01.

The comparison results of Na^+ air concentration, calculated with the EMEP model using the five source functions, with observations at the individual EMEP stations are provided in Appendix (Table A2). On average, M&M yields the best agreement with observed Na^+ in terms of bias and correlation, i.e. it gives the best temporal correlation between calculated and measured Na^+ (0.58) and next to the best bias of +23.

ACPD
11, 11143–11204, 2011

7.2 Effect of meteorology

Calculated emission rates of sea salt crucially depend on the wind speed, so that even a small incorrectness in wind speed data can result in quite wrong predictions of sea salt fluxes. To see how different meteorological input affects calculated sea salt, model runs have been performed with different meteorological drivers, i.e. PARLAM-PS, HIRLAM version 7.1 and ECMWF models. The results of the runs and comparison with observations at EMEP sites are summarised in Table 7.

Compared with Na^+ measurements, there is a certain improvement in model calculated sea salt concentrations using HIRLAM-v7.1 and ECMWF (IFS) meteorology. The positive bias decreases from 12 (PARLAM-PS) to 4 and 0%, and the spatial correlation improves from 0.69 (PARLAM-PS) to 0.83 and 0.82 respectively. Also, different sea salt seasonal variation is predicted using different meteorological data. PARLAM-PS and HIRLAM give somewhat larger seasonal variability compared to observations, while flatter seasonality is calculated with ECMWF meteorology.

Unfortunately, verification of wind speed from PARLAM-PS, HIRLAM and ECMWF (IFS) is only available over land, where PARLAM-PS is unfavourably characterised with the largest mean absolute error and its standard deviation. Beside the wind speed, also other meteorological parameters modify sea salt concentrations and distribution. In particularly, precipitation has significant effect on airborne sea salt, efficiently scavenging the aerosols.

7.3 Effect of wet deposition

As shown above, Na^+ concentrations in precipitation are considerably underestimated by the model, while Na^+ air concentrations are slightly overestimated for all sea salt source functions tested. To see what processes could be responsible for those discrepancies, we have tested the possibility of model (1) underestimating wet scavenging of sea salt and (2) calculating too efficient dry deposition of sea salt. The results

ACPD
11, 11143–11204, 2011

of sensitivity tests of calculated sea salt concentrations to removal processes are presented in the following sections.

Being very hygroscopic, sea salt aerosols are efficiently removed from the clouds by rain drops. Most sea salt rainout takes place in the lower part of the cloud, where the precipitation intensity is the largest. The washout below clouds depends on the aerosol size and is much more efficient for coarse sea salt than for fine sea salt. In the model, the below-cloud scavenging is about 2.5 times less efficient for coarse sea salt and as much as 10 times less efficient for fine sea salt compared to in-cloud rainout. On the other hand, relatively more sea salt mass is found in the lower altitudes, likely below the clouds, especially over the source regions.

Sensitivity tests have been performed for both in-cloud and below-cloud scavenging of sea salt. The model's wet deposition scheme uses scavenging ratios to calculate aerosol removal from the cloud layers. In the base runs presented in the previous sections, the scavenging ratio $W = 1 \times 10^6$ was used. To investigate the effect of wet scavenging ratio on calculated Na^+ concentrations, additional calculations have been performed using $W = 1.6 \times 10^6$ and 2×10^6. The increase of scavenging ratio by factors of 1.6 and 2 results in a rather modest decrease of Na^+ in air (with model bias changing from 12% to 5% and −1%, respectively) and in an insignificant or no increase in Na^+ in precipitation (Table 8). This is probably because the efficiency of sea salt scavenging in clouds is already so high, that most of aerosol mass gets rained out anyway; hence the further increase of scavenging ratio appears to add only very little to scavenged sea salt mass. The effect of increasing wet scavenging ratio appears less pronounced in the most remote from sea sites, since most of sea salt particles likely get scavenged before they reach the in-land sites. Further increase of scavenging ratio causes in fact a decrease in wet deposition of sea salt over land, as even a greater portion of sea spray is removed by precipitation already over oceans.

Further, we have increased the below-cloud washout efficiency to 1.0 from 0.4 and 0.8 for fine and coarse aerosols respectively. As a result, the positive bias for Na^+ in air is eliminated, but the negative bias for Na^+ in precipitation gets even larger (Table 8).

ACPD
11, 11143–11204, 2011

Also in this case, more efficient wet scavenging of sea salt means that more of it is removed from the air over the oceans, resulting in overall lower Na^+ concentrations in air and precipitation over land.

7.4 Effect of dry deposition

Hypothesizing that too efficient dry deposition in the model could remove too much sea salt mass from air during dry periods and contribute to the underestimation of Na^+ in precipitation, we have looked at the effect of dry deposition reduction. A model run has been made where dry deposition velocity was decreased by 50%. This has increased Na^+ concentrations in air by 48% and Na^+ concentrations in precipitation by 38% on average at the EMEP sites. In this test, the model overestimates Na^+ in air by 66%, whereas it still underestimates Na^+ in precipitation by 51% (Table 8). It can be noted that the reduction of dry deposition velocity is found to cause the greatest increase in calculated Na^+ air concentrations for in-land sites.

7.5 Effect of sea surface roughness

Another parameter effecting sea salt production is the roughness of sea, which is described through Charnock's constant β (Eq. 5). The value of β has recently been changed from 0.032 to 0.00114 which is considered to be more consistent with the present description of boundary layer processes in the EMEP model. A smaller value of β means a less rough sea and a larger wind speed at 10 m height which, in turn, increases the fluxes of sea spray.

The sensitivity tests show that on average, the calculated sea salt concentrations are only 5% lower when using $\beta = 0.032$ compared to $\beta = 0.0114$, with somewhat larger difference in winter and spring. This slightly decreases model's bias from 12 to 7% compared against Na^+ observations in 2006. The correlation between calculated and observed Na^+ does not appear to be affected by varying Charnock's parameter.

ACPD
11, 11143–11204, 2011

7.6 Including larger sea salt particles

Discrepancies between calculated and measured sea salt concentrations can occur due to inconsistency in the upper "cut-off" size of sea salt aerosols. The standard EMEP model is set up to calculate approximately $PM_{2.5}$ and PM_{10}. The upper dry diameter of generated sea salt particle is set to 5 µm, which would correspond to aerosol ambient diameters between 7.5 and 10.6 µm at relative humidity between 40 and 80%. As said in Sect. 4, filter-pack samplers collect particles with aerodynamic diameters of approximately 10 µm at ambient conditions, though there is no defined cut-off size. For sampled Na^+ in precipitation, there is practically no cut-off size for collected sea salt aerosols. Some amount of sea salt particles larger that e.g. 10 µm can as well be present in the air and when scavenged, they will contribute to Na^+ concentrations in precipitation. The fraction of sea salt particles larger than 10 µm will considerably decrease with the distance from the sea coast due to their fast gravitational settling. Therefore the effect of not accounting for those "giant" sea salt aerosols is expected to be more pronounced at the sites close to the sea shore than at in-land sites.

To estimate the contribution of sea salt particles larger than 10 µm to Na^+ concentrations, a new model run for 2006 has been performed, in which sea salt aerosols with dry diameters up to 17 µm were included. For Na^+ in air, these results overestimate measured concentrations by 46% (as compared to 12% in the base run) (Table 9). As expected, somewhat greater increase in calculated Na^+ is seen for the sites close to the sea coasts (not shown). The negative bias for Na^+ in precipitation is only reduced to −51% compared to −64% in the base run.

7.7 Unaccounted processes

Water salinity. The content of salt in oceanic surface water varies from below 10‰ in the Baltic Sea and about 18‰ in the Black Sea to above 37‰ in the middle of NE Atlantic and 38‰ in the Mediterranean Sea. There are experimental indications that water salinity can affect the generation of sea salt. Mårtinsson et

ACPD
11, 11143–11204, 2011

al. (2003) measured that for aerosols smaller than 0.2 µm salinity did not affect the original droplet number production, but only the size distribution of dry sea salt particles. However for larger aerosols, the total volume of generated sea spray droplets increases with an increase of water salinity. From their experiments, sea salt concentrations at salinity 37‰ were about an order of magnitude larger than those at salinity 9.2‰. In this work, an average water salinity of 33‰ is assumed, according to parameterisation by Mårtinsson et al. (2003). The first known to us attempt to include effect of water salinity on sea spray production has been made by Sofiev et al. (2011), based on laboratory measurements from Mårtinsson et al. (2003).

Surf zone. Based on field measurements, de Leeuw et al. (2000) estimated that sea spray production could be a factor of 2 greater in surf zone compared to the open ocean. An accurate accounting for sea spray contribution from a surf zone in the regional model is not a trivial task, as it requires gridding of the surface zone. Since the surf zone is rather narrow, its relative area within the EMEP 50×50 km^2 grid cell will be quite small. Also, Gong et al. (2002) showed that surf zone sea spay flux was much smaller compared to that for an open ocean and thus concluded that the surfing contribution to the total sea salt production was negligible. We are not aware of any regional/global model including presently this effect in calculations.

8 Comparison of sea salt from EMEP and SILAM model

Results for sea salt from the EMEP model are compared with those from SILAM model (Sofiev et al., 2006) for the year of 2007.

ACPD
11, 11143–11204, 2011

8.1 Sea salt description in the SILAM model

SILAM's sea salt emission parameterisation development was based on the parameterisation of Monahan et al. (1986) and the data of Mårtensson et al. (2003), which were combined into a unified set of functions (Sofiev et al., 2011). This parameterisation takes into account effects of wind speed, salinity, and water temperature and covers sea salt particles with dry diameter from 20 nm to 10 µm.

The sea salt production term is taken as a product of a size-distribution shape function and the forcing terms (some of them also related to particle size):

$$\frac{dF}{dd_d} = W\,(U_{10})\frac{dF_0}{dd_d}\,(d_d)\,F_{TW}\,(d_d,\,T_w)\,F_{SW}(d_d,S_w) \tag{6}$$

Here, F is the flux of sea salt particles per unit range of the particle size, W, F_0, F_{TW}, F_{SW} are the wind forcing, the shape function, the water-temperature correction, and the water-salinity correction terms respectively, T_w and S_w is the sea water temperature and salinity, and d_d is the dry diameter.

The wind forcing, same as in the EMEP model, is expressed as a fraction of water area covered by white caps for specific wind speed at 10 m height $U_{10\ m}$ (Monahan and O'Muircheartaigh, 1980):

$$W\,(U_{10}) = 3.84\times10^{-6}U_{10}^{3.41} \tag{7}$$

The Monahan et al. (1986) describes a source function for the production of sea salt aerosol in the d_d size range from about 0.9 µm up to about 8 µm. Observations extracted from the Mårtensson et al. (2003) paper for sea water surface temperature 298 K and sea water salinity 33‰ were used to extrapolate M86 to particle sizes down to 20 nm. This resulted in a single source function for particles with diameters from 20 nm to 10 µm for these reference conditions:

$$\left(\frac{dF_0}{dd_d}\right)_{33,\ 25^\circ} = 6.9\times10^5\times\frac{\exp\left(-{}^{0.12}/_{d_d}\right)}{0.05+\exp\left(-{}^{0.1}/_{d_d}\right)}\times\frac{1+0.05d_d^{1.05}}{d_d^3}\times10^{1.6\exp\left(-\left(\frac{1.1\log d_d}{0.8}\right)^2\right)} \tag{8}$$

ACPD
11, 11143–11204, 2011

To calculate sea salt production for other water temperatures and salinities, correction factors are applied which were derived based on the experimental data of Mårtensson et al. (2003). The full description of the parameterisation in the SILAM model can be found in Sofiev et al. (2011).

For this study, sea salt in five size fractions has been calculated, i.e. for dry diameters in the ranges 0.01–0.1, 0.1–1.0, 1.0–2.5, 2.5–10, and 10–30 µm. The computations with SILAM have been performed with meteorological fields from the European Centre for Medium-Range Weather Forecasts (ECMWF) at the grid of 20 × 20 km^2. Compared to the EMEP calculation domain, SILAM's grid covers somewhat a smaller area of the North Atlantic Ocean, starting at 17° W and 33° N (left lower corner).

8.2 Comparison of results

Air concentrations of Na^+ calculated with the EMEP and the SILAM models have been compared with EMEP measurements in 2007. Na^+ concentrations have been derived as 31% of the mass of sea salt concentrations. In addition to differences in the formulation of sea spray generation, sea salt aerosols are treated differently in the models. The SILAM model transports sea salt in each of the five size fractions individually, while the EMEP model aggregates sea salt in two, the fine and the coarse, fractions. For comparison with observations, sea salt aerosols in the first four size fractions (up to 10 µm of dry diameter) from the SILAM model have been included, whereas sea salt aerosols up to about 10 µm of ambient diameter in the EMEP model have been considered. Furthermore, different meteorological drivers have been used in the runs, namely ECMWF model for the SILAM and HIRLAM model for EMEP. It should also be noted that SILAM calculations have been performed at a fine resolution of 20 × 20 km^2 compared to EMEP calculations at 50 × 50 km^2. Given typically large sea salt gradients, the SILAM model, due to its better resolution, is expected to be more capable of reproducing observed concentrations, in particular at the sites in close proximity to the sea.

ACPD
11, 11143–11204, 2011

Figure 8 compares Na^+ air concentrations from the EMEP and SILAM models with observed values, ranking the sites according to decreasing measured concentrations (crudely representing the increasing distance from the sea coast). Scatter-plots for calculated versus observed Na^+ air concentrations are shown in Fig. 9, and the results of statistical analysis are summarised in Table A3. Both models reproduce realistically the observed distribution of sea salt concentrations. The spatial correlation between calculated and measured Na^+ is 0.73 for EMEP and 0.78 SILAM calculations. For about two third of the sites, the models calculate quite close Na^+ concentrations, whereas significant discrepancies are found for Finnish and Irish stations. Both models somewhat underestimate Na^+ concentrations at about 70% of the sites, with largest underestimation at coastal Irish site IE08. Both models considerably overestimate Na^+ at Norwegian sites NO15 and NO39 (SILAM also overestimates at NO01 and NO55). Large overestimation by the EMEP model of Na^+ at FI09 and FI17 can partly be explained by that it does not account for the effect of sea water salinity on sea spray generation, whereas the SILAM model does. A simple model test, in which sea spray production from the Baltic Sea is reduced by a factor of five, gives reductions of biases from 498 to 200% at FI09 and from 128% to 15% at FI11. Another reason for those overestimations is probably a relatively coarse resolution of the EMEP model. The site FI09 is situated on a small island which area occupies less than 1% of the EMEP grid cell and thus the observations are not representative for the whole of $50 \times 50\,km^2$ grid cell. Similarly, the site FI17 is not quite representative, as it is located in the very corner of a grid cell, which has 69% of its area covered by the Baltic Sea. Calculated Na^+ concentrations drop from $0.51\,\mu g\,m^{-3}$ to $0.15–0.2\,\mu g\,m^{-3}$ in the adjacent grids, which agrees better with observed value.

The temporal correlation between calculated and measured daily Na^+ air concentrations is quite variable for both models. On average, the correlation tends to be somewhat better for the sites at short and medium distances from the sea compared to in-land sites. In general, the EMEP model shows correlation better than SILAM at Danish, Finnish and Slovakian sites, while Na^+ from SILAM correlates better with

ACPD
11, 11143–11204, 2011

observations at some of the German, Austrian and some of the Norwegian and Irish sites (Table A3). The differences between models' temporal correlations with measurements are most probably due to differences in the wind fields from the HIRLAM and ECMWF models used in EMEP and SILAM calculations.

9 Summary and outlook

We have used the EMEP Unified model (version rv3.1) to calculate sea salt concentrations and depositions over Europe. The ability of the model to reproduce sea salt observations for multiple years has been analysed, focusing on studying the effects of uncertainties in sea salt production and lifetime on model results.

As a part of the uncertainty study, a series of model calculations has been performed using different source functions for sea spray production. Based on a critical review of the documentation available in scientific literature, several sea spray source functions have been selected for our study, i.e. those from Mårtensson et al. (2003), Monahan et al. (1986), Andreas (1998), Smith and Harrison (1998), Vignati et al. (2001), Gong (2003) and Clarke et al. (2006). Prior to regional computations, the behaviour of those selected source functions has been studied using a box-model. The box-model study has allowed identifying the differences between the source function in their description of the wind speed dependence of sea salt fluxes and the size distribution of generated sea salt aerosols. The main findings are:

- the largest discrepancies between the source functions are found in sea spray fluxes for droplets with r_{80} smaller than 0.1 µm (up to two orders of magnitude);
- at wind speed of 10 m s^{-1}, M&M number and volume fluxes of sea spray are larger than those from G03 and V01 for droplets smaller than about 2 µm. M&M and G03 fluxes are quite close for sea spray larger than about 0.4 µm for all wind speeds, while for smaller droplets fluxes from M&M are larger than those from G03. A98

ACPD
11, 11143–11204, 2011

fluxes differ significantly from the other source functions, greatly underestimating fluxes of the smallest droplets;

- the dependence on wind speed for M&M and G03 fluxes is stronger compared to V01, so that for low winds V01 calculates close to or larger sea spray fluxes compared to M&M and G03;
- M&M and C06 show similar wind dependences of sea spray flux, but the size distribution of sea spray droplets from those schemes are different, namely C06 calculates smaller fluxes of sea salt aerosols below r_{80} of 0.2 µm, but larger fluxes for larger droplets compared to M&M.

Further, the sea salt source functions have been tested within the regional EMEP model. EMEP model calculations for 2006 show that the largest sea salt concentrations are produced by C06 source function following by those calculated using V01, while SH98 parameterisation gives the lowest sea salt concentrations. Lying between those upper and lower estimates, sea salt concentrations from M&M (combination of Monahan et al. (1986) and Mårtensson et al. (2003) source functions) and G03 are quite close, whereas results given by A98 are somewhat lower.

Compared to EMEP observations for 2006, M&M and G03 parameterisations give quite similar results, overestimating annual mean Na^+ air concentrations by 12 and 25% respectively. A98 and SH98 underestimate Na^+ air concentrations on average by 10 and 40% respectively. V01 parameterisation overestimates observed Na^+ by as much as 120%, whereas Na^+ air concentrations obtained with C06 exceed measured values by almost an order of magnitude. The spatial correlation between annual mean calculated and measured Na^+ concentrations is quite similar for all parameterisations, with the correlation coefficient ranging between 0.76 for SH98 and 0.79 for M&M. There are also seasonal differences in the model performance when different source functions are used. At individual measurement sites, the temporal correlations are the best for M&M source function, closely followed by G03 and SH98, and considerably lower correlation is found for A98 and V01. The results in terms of model bias are somewhat

ACPD
11, 11143–11204, 2011

variable. On average for all sites, M&M shows the most promising results providing the best temporal correlation between calculated and measured Na^+ (0.58) and next to the best bias of +23.

Compared to Na^+ measurements from the EMEP network, the EMEP model shows a reasonable performance for Na^+ air concentrations for years 2004 through 2007. On the other hand, Na^+ in precipitation is under-predicted, especially in the seasons outside summer and particularly in winter. A series of performed tests has not given us a clear answer regarding the reason for this underestimation. The model reproduces the distribution of Na^+ over land fairly well, with spatial correlation varying between 0.76 and 0.81 for air concentrations and between 0.70 and 0.91 for Na^+ in precipitation for different years. The model is doing quite good job of capturing sea salt episodes as indicated by temporal correlation coefficients, lying between 0.5 and 0.8 at most of the sites for the period from 2004 to 2007.

Comparison with data from EMEP intensive measurement periods at four selected sites in June 2006 and January 2007 suggests that model calculated production of sea salt mass may be too small in summer, while less so in winter. The results also indicate the possibility of too efficient removal of sea salt aerosol from the air, as calculated Na^+ air concentrations tend to be greater under-predicted at the sites farther from the sea. On average, model calculated distribution of sea salt mass between fine and coarse aerosols is quite close to observed. However for some sites, the model allocates more Na^+ in the fine fraction in summer compared to winter which is not seen in the measurement data. This implies that wind speed dependence of sea spray flux size distribution in the M&M parameterisation needs further testing and evaluation.

A series of sensitivity tests has been carried out to study the effect of the uncertainties in different parameters and prosesses on model results for sea salt versus measurements. Sea salt results are shown to be sensitive to changing the meteorological driver, in particular due to changes in wind speed and precipitation data. Sea salt concentrations calculated with the EMEP model improve when using HIRLAM-v7.1 and ECMWF (IFS) meteorology compared to those using the older NWP model,

ACPD
11, 11143–11204, 2011

PARLAM-PS. Furthermore, some hypotheses have been tested regarding possible reasons for a considerable underestimation by the EMEP model of Na^+ in precipitation. Increasing in-cloud scavenging ratio by a factor of two or increasing below-cloud scavenging efficiency to 100% results in nearly unbiased model calculated Na^+ in air, whereas the obtained increase in Na^+ in precipitation (and Na^+ wet deposition) is negligible. Furthermore, some moderation of model underestimation of Na^+ in precipitation is achieved by reducing dry deposition velocity by half, but Na^+ in air becomes far too high in this case. Finally, accounting for the contribution from sea salt particles larger than 10 µm (up to approximately 25–30 µm) in addition to increased wet scavenging, allows achieving only a rather small reduction of model underestimation of Na^+ in precipitation. Thus, underestimation of Na^+ in precipitation and Na^+ wet deposition by the model still remains unexplained and requires further investigation.

Sea salt calculations with the EMEP model have been compared to results from the SILAM model and observations for 2007. Both models are found to realistically reproduce observed distribution of sea salt concentrations, with the spatial correlation between calculated and measured Na^+ of 0.73 for EMEP and 0.78 for SILAM. For about two third of the sites, the models calculate quite close Na^+ concentrations, whereas significant discrepancies are found for Finnish and Irish stations strongly influenced by sea spray. Both models somewhat underestimate Na^+ concentrations at about 70% of the sites, with the largest underestimation at coastal Irish site IE08. The temporal correlations between calculated and measured daily Na^+ air concentrations are quite variable for both models, and tend to be somewhat better for the sites at short and medium distances from the sea compared to in-land sites. Differences in calculated sea salt are explained to be due to different parameterisations of sea spray production and the following treatment of sea salt aerosols by the models, as well as due to the use of different meteorological drivers for models' simulations. Moreover, the discrepancies in models' results compared to observations can partly be due to different grid resolutions used in model calculations, i.e. $50 \times 50\,km^2$ for EMEP and $20 \times 20\,km^2$ for SILAM.

ACPD
11, 11143–11204, 2011

The future work on improving sea salt modelling will facilitate improvement of nitrate chemistry in the EMEP model, namely formation of coarse nitrate associated with sea salt. Some work has already been done to include a kinetic parameterisation to describe the uptake of HNO_3 on sea salt aerosols and its further reaction of with NaCl to form coarse $NaNO_3$ particles (Berge, 2009). First results showed improvements of correlation between calculated and observed nitrate for several EMEP stations, which was very promising, however, the concentrations of coarse nitrate was underestimated. Further work is envisaged to carry out more testing against observations and to improve the scheme for nitrate formation on sea salt in the EMEP model. Providing a better insight on model's ability to reproduce sea salt for Europe and uncertainties associated with sea salt calculations, this work contributes to further improvement of EMEP aerosol modelling.

Acknowledgements. The authors are grateful to Perrino S. at C. N. R. Institute of Atmospheric Pollution and Makkonen U. at the Finnish Meteorological Institute for intensive measurement data used in this work.

References

Andreas, E. L.: A new sea spray generation function for wind speeds up to 32 m s^{-1}, J. Phys. Oceanogr., 28(11), 2175–2184, 1998.

Andreas, E. L., Pattison, M. J., and Belcher, S. E.: "Production rates of sea-spray droplets", in: Clarification and elaboration, edited by: Pattison, M. J. and Belcher, S. E., J. Geophys. Res., 106(C4), 7157–7161, 2001.

Athanasopoulou, E., Tombrou, M., Pandis, S. N., and Russell, A. G.: The role of sea-salt emissions and heterogeneous chemistry in the air quality of polluted coastal areas, Atmos. Chem. Phys., 8, 5755–5769, doi:10.5194/acp-8-5755-2008, 2008.

Berge, H.: Implementation and evaluation of a parameterisation of coarse nitrate, Master Thesis in Geoscience, Meteorology and Oceanography, University of Oslo, Department of Geoscience, Oslo, Norway, 2009.

ACPD

11, 11143–11204, 2011

Blomqvist, G. and Johansson, E.-L.: Airborne spreading and deposition of de-icing salt – a case study, The Science of The Total Environment, 235,(1–3), 161–168, 1999.
Clarke, A. D., Owens, S. R., and Zhou, J.: An ultrafine sea-salt flux from breaking waves: Implications for cloud condensation nuclei in the remote marine atmosphere, J. Geophys. Res., 111, D06202, doi:10.1029/2005JD006565, 2006.
De Leeuw, G., Neele, F. P. Hill, M., Smith, M. H., and Vignati, E.: Production of sea spray aerosol in the surf zone, J. Geophys. Res., 105(D24), 29397–29409, 2000.
EC Directive 2008/50/Ec of the European Parliament and of the council of 21 May 2008 on ambient air quality and cleaner air for Europe: available at: http://ec.europa.eu/environment/air/legis.htm (last access: April 2011), 2008.
EMEP/CCC: Manual for sampling and chemical analysis, Revised November 2001, Norwegian Institute for Air Research Kjeller, EMEP/CCC-Report 1/95, available at: http://tarantula.nilu.no/projects/ccc/manual/index.html (last access: April 2011), 1995.
Erickson, D. J. and Duce, R. A.: On the global flux of atmospheric sea salt, J. Geophys. Res., 93, 14079–14088, 1988.
Fagerli, H., Simpson, D. and Tsyro, S.: Unified EMEP model: Updates, in Transboundary acidification, eutrophication and ground level ozone in Europe, EMEP Status Report 1/2004, Norwegian Meteorological Institute, Oslo, Norway, 11–18, 2004.
Foltescu, V. L., Pryor, S. C., and Bennet, C.: Sea salt generation and removal on the regional scale, Atmos. Environ., 39, 2123–2133, 2004.
Hjellbrekke, A.-G. and Fjæraa, A. M.: Data Report 2007 Acidifying and eutrophying compounds and particulate matter, EMEP/CCC-Report 1/2009, Norwegian Institute for Air Research, Kjeller, 2009.
Garratt, J. R.: The atmospheric boundary layer, Cambridge University Press, 1992.
Geever, M., O'Dowd, C. D., van Ekeren, S., Flanagan, R., Nilsson, E. D., de Leeuw, G., and Rannik, U.: Submicron sea spray fluxes, Geophys. Res. Lett., 32, L15810, doi:10.1029/2005GL023081, 2005.
Gerber, H. E.: Relative-humidity parameterisation of the Navy aerosol model (NAM), NRL Rep. 8956, Natl., Res. Lab., Washington, DC, 1985.
Grini, A., Myhre,G., Sundet, J. K., and Ivar S. A. Isaksen: Modelling the annual cycle of sea salt in the global 3-D model OSLO CTM-2, Concentrations, fluxes, and radiative impact, J. Clim., 15, 1717–1730, 2002.
Gong, S. L.: A parameterisation of sea-salt aerosol source function for sub- and super-micron

ACPD
11, 11143–11204, 2011

particles, Glob. Biogeochem. Cyc., 17(4), 1097, doi:10.1029/2003GB002079, 2003.
Gong, S. L., Barrie, L. A., and Blanchet, J.-P.: Modeling sea-salt aerosols in the atmosphere: 1, Model development, J. Geophys. Res., 102, 3805–3818, 1997a.
Gong, S. L., Barrie, L. A., Prospero, J. M., Savoie, D. L., Ayers, G. P., Blanchet, J.-P., and Spacek, L.: Modeling sea-salt aerosols in the atmosphere: 2, Atmospheric concentrations and fluxes, J. Geophys. Res., 102, 3819–3830, 1997b.
Gong, S. L., Barrie, L. A., and Lazare, M.: Canadian Aerosol Module(CAM): A size-segregated simulation of atmospheric aerosol processes for climate and air quality models, 2, Global sea-salt aerosol and its budgets, J. Geophys. Res., 107(D24), 4779, doi:10.1029/2001JD002002, 2002.
Guelle, W., Schulz, M., Balkanski, Y., and Dentener, F.: Influence of the source formulation on modeling atmospheric global distribution of sea salt aerosol, J. Geophys. Res., 106(D21), 27509–27524, 2001.
Hellsten, S., van Loon, M., Tarrason, L., Vestreng, V., Tørseth, K., Kindbom, K. and Aas, W.: Base cations deposition in Europe, IVL Report B1722, Swedish Environmental Research Institute, Stockholm, available at: http://www3.ivl.se/rapporter/pdf/B1722.pdf, 2007.
Langmann, B., Varghese, S., Marmer, E., Vignati, E., Wilson, J., Stier, P., and O'Dowd, C.: Aerosol distribution over Europe: a model evaluation study with detailed aerosol microphysics, Atmos. Chem. Phys., 8, 1591–1607, doi:10.5194/acp-8-1591-2008, 2008.
Lewis, E. R. and Schwartz, S. E.: Sea Salt Aerosol Production: Mechanisms, Methods, Measurements, and Models: A Critical Review, American Geophysical Union, Washington, DC, 2004.
Liu, H., Crawford, J. H., Pierce, R. B., Norris, P., Yantosca, R. M., Evans, M. J., Kittaka, C., Feng, J., and Tie, X: Radiative effect of clouds on tropospheric chemistry in a global three-dimensional chemical transport model, J. Geophys. Res., 111, D20303, doi:10.1029/2005JD006403, 2006.
Ma, X., von Salzen, K., and Li, J.: Modelling sea salt aerosol and its direct and indirect effects on climate, Atmos. Chem. Phys., 8, 1311–1327, doi:10.5194/acp-8-1311-2008, 2008.
Maykut, N., Lewtas, J., Kim, E., and Larson, T. V.: Source apportionment of $PM_{2.5}$ at an urban IMPROVE site in Seattle, Washington, Environmental Science and Technology, 37, 5135–5142, 2003.
Millero, F. J.: Physicochemical controls on seawater, in: Treatise on Geochemistry, edited by: Holland, H. D. and Turkian, K. K., Elsevier, Amsterdam, 2004.

ACPD
11, 11143–11204, 2011

Monahan E. C. and O'Muircheartaigh, I.: Optimal power-law description of oceanic whitecap coverage dependence on wind speed, J. Phys. Oceanogr., 10, 2094–2099, 1980.
Monahan, E. G., Spiel, D. E., and Davidson, K. L.: A model of marine aerosol generation via whitecaps and wave disruption, in: Oceanic Whitecaps, edited by: Monahan, E. and Niocaill, G. M., 167–174, D. Reidel, Norwell, Mass., 1986.
Mårtensson, E. M., Nilsson, E. D., de Leeuw, G., Cohen, L. H., and Hansson, H.-C.: Laboratory simulations and parameterisation of the primary marine aerosol production, J. Geophys. Res., 108(D9), 4297, doi:10.1029/2002JD002263, 2003.
O'Dowd, C. D., Smith, M. H., Costerdine, I. E., and Lowe, J. A.: Marine aerosol, sea salt, and the marine sulphur cycle: A short review, Atmos. Environ., 32, 73–80, 1997.
Ooki, A., Uematsu, M., Miura, K. and Nakae, S.: Sources of sodium in atmospheric fine particles, Atmos. Environ., 36, 4367–4374, 2002.
Pierce, J. and Adams, P. J.: Global evaluation of CCN formation by direct emission of sea salt and growth of ultrafine sea salt, J. Geophys. Res., 111, D06203, doi:10.1029/2005JD006186, 2006.
Pryor, S. C., Barthelmie, R. J., Schoof, J. T., Binkowski, F. S., Delle Monache, L., and Stull, R.: Modeling the impact of sea-spray on particle concentrations in a coastal city, Sci. Total Environ., 391(1), 132–142, 2008.
Schulz, M., de Leeuw, G., and Balkanski, Y.: Sea salt aerosol source functions and emissions, in: Emissions of Atmospheric Trace Components, edited by: Granier, C., Artaxo, P., and Reeves, C. E., 333–359, Kluwer Academic Publishers, 2004.
Sellegri, K., Gourdeau, J., Putaud, J. P., and S. Despiau: Chemical composition of marine aerosol in a Mediterranean coastal zone during the FETCH experiment, J. Geophys. Res., 106, 12023–12037, available at: http://www.agu.org/journals/jd/v106/iD11/2000JD900629/2000JD900629.pdf, 2001.
Simpson, D., Fagerli, H., Jonson, J. E., Tsyro, S., Wind, P., and Tuovinen, J.-P.: Transboundary Acidification, Eutrophication and Ground Level Ozone in Europe, Part I, Unified EMEP Model Description, EMEP/MSC-W Status report 1/2003 Part I, Norwegian Meteorological Institute, Oslo, Norway, available at: http://www.emep.int, 2003.
Smith, M. H. and Harrison, N. M.: The sea spray generation function, J. Aerosol Sci., 29, Suppl. 2, 189–190, 1998.
Smith, M. H., Park, P. M., and Consterdine, I. E.: Marine aerosol concentrations and estimated fluxes over sea, Q. J. R. Meteorol. Soc., 119, 809–824, 1993.

ACPD
11, 11143–11204, 2011

Sofiev, M., Siljamo, P., Valkama, I., Ilvonen, M., Kukkonen, J.: A dispersion modelling system SILAM and its evaluation against ETEX data, Atmos. Environ., 40, 674–685, doi:10.1016/j.atmosenv.2005.09.069, 2006.
Sofiev, M., Soares, J. Prank, M. de Leeuw, G., and Kukkonen, J.: A regional-to-global model of emission and transport of sea salt particles in the atmosphere, in preparation, 2011.
Stier, P., Feichter, J., Kinne, S., Kloster, S., Vignati, E., Wilson, J., Ganzeveld, L., Tegen, I., Werner, M., Balkanski, Y., Schulz, M., Boucher, O., Minikin, A., and Petzold, A.: The aerosol-climate model ECHAM5-HAM, Atmos. Chem. Phys., 5, 1125–1156, doi:10.5194/acp-5-1125-2005, 2005.
Stull, R. B.: An Introduction to Boundary Layer Meteorology, Atmospheric Science Library, Kluwer Academic Publishers, 1988.
Tsyro, S.: Regional Model for Formation, Dynamics, and Long-range Transport of Atmospheric Aerosol, Russian Meteorology and Hydrology, 33(2), 82–90, 2008.
Tsyro, S., Berge, H., Benedictow, A., and Gauss, M.: Studying the effect of meteorological input on Unified EMEP model results, in: Transboundary acidification, eutrophication and ground level ozone in Europe in 2008, EMEP Status Report 1/2010, Norwegian Meteorological Institute, Oslo, Norway, available at: http://www.emep.int, 2010,
van Loon, M., Tarrasón, L. and Posch, M.: Modelling Base Cations in Europe, MSC-W Technical Report 2/05, Norwegian Meteorological Institute, Oslo, Norway, 2005.
Uggerud, H. and Hjellbrekke, A.-G.: The twenty-sixth intercomparison of analytical methods within EMEP, Norwegian Institute for Air Research, Kjeller, EMEP/CCC-Report 6/2009, 2009.
van den Berg, A., Dentener, F., and Lelieveld, J.: Modeling the chemistry of the marine boundary layer: Sulphate formation and the role of sea-salt aerosol particles, J. Geophys. Res., 105(D9), 11671–11698, doi:10.1029/1999JD901073, 2000.
Vignati, E., de Leeuw, G., and Berkowicz, R.: Modeling coastal aerosol transport and effects of surf-produced aerosols on process in the marine atmospheric boundary layer, J. Geophys. Res., 105(D17), 20225–20238, 2001.
White, W. H.: Chemical markers for sea salt in IMPROVE aerosol data, Atmos. Environ., 42, 261–274, 2009.
Zakey, A. S., Giorgi, F., and Bi, X.: Modelling of se salt in a regional climate model: Fluxes and radiative forcing, J. Geophys. Res., 113, D14221, doi:10.1029/2007JD009209, 2008.

ACPD
11, 11143–11204, 2011

Table 1. Size fractions used for calculations of sea spray production in the EMEP model: shown are the borders for dry diameters (d_{dry} in µm).

d_{dry}	0.02	0.05	0.10	0.145*	0.25	0.419*	0.60	1.25	1.6	3.0	5.0	10	17

* Chosen in order to comply with formula from Mårtensson et al. (2003).
Here, light-grey and black colours mark the fine and the coarse sea salt aerosols, which are included in standard calculations; the size fractions in grey boxes have been used for test runs.

ACPD
11, 11143–11204, 2011

Table 2. Comparison statistics between calculated and observed Na^+ concentrations in air and precipitation and Na^+ wet deposition.

	2004	2005	2006	2007*
Na^+ air				
N_{sites}	11	17	22	26
Bias (%)	46	22	12	8
R	0.78	0.81	0.79	0.76
RMSE	0.39	0.56	0.61	0.65
Na^+ precip				
N_{sites}	31	32	38	40
Bias (%)	−63	−66	−64	−73
R	0.73	0.70	0.93	0.77
RMSE	1.62	1.67	0.65	2.98
Na^+ w. dep				
Bias (%)	−69	−76	−77	−72
R	0.87	0.92	0.71	0.89

* Note that HIRLAM 7.1 version was used for 2007 model calculations, while meteorology for 2004–2006 is based on PARLAM-PS.

ACPD
11, 11143–11204, 2011

Table 3. Seasonal comparison between calculated and observed Na^+ concentrations in air and precipitation for the period 2004-2007 (also bias for precipitation is shown in the last column).

	Na^+ in air				Na^+ in prec				Prec
Seasons	Obs	Mod	Bias	Corr	Obs	Mod	Bias	Corr	Bias
JF	1.00	1.16	25	0.64	2.57	0.70	−70	0.34	13
MAM	0.70	0.85	27	0.66	1.37	0.42	−69	0.45	9
JJA	0.54	0.60	13	0.61	0.77	0.26	−65	0.41	−4
SON	0.78	0.93	23	0.68	1.44	0.49	−67	0.42	−2

ACPD
11, 11143–11204, 2011

Table 4. Average observed (Obs) and modelled (Mod) concentrations of Na^+ in PM_{10} and $PM_{2.5}$ and correlation coefficient (Corr) for EMEP intensive periods in June 2006 and January 2007.

		June 2006		January 2007	
		Na_PM_{10}	$Na\_PM_{2.5}$	Na_PM_{10}	$Na\_PM_{2.5}$
NO01	Obs	0.39	0.12	0.45	0.34
	Mod	0.28	0.12	0.54	0.18
	Corr	0.67	0.46	0.33	0.48
FI17	Obs	0.21	0.12	0.27	0.12
	Mod	0.23	0.09	0.39	0.09
	Corr	0.40	0.88	0.79	0.76
IT01	Obs	0.38	0.14	0.91	0.17
	Mod	0.11	0.04	0.68	0.19
	Corr	−0.25	0.04	0.52	0.13
DE44	Obs	0.28	0.10	0.64	0.26
	Mod	0.12	0.06	0.51	0.18
	Corr	0.88	0.81	0.68	0.63

ACPD
11, 11143–11204, 2011

Table 5. Comparison statistics for annual mean calculated Na^+ air concentrations and observations in 2006, obtained with the EMEP model, using M&M, G03, A98, SH98 and V01 source functions.

	EMEP (M&M)	G03	A98	SH98	V01
N_{sites}	22	22	22	22	22
Bias	12	25	−10	−40	120
R	0.79	0.78	0.77	0.76	0.77
RMSE	0.61	0.70	0.58	0.70	1.65

ACPD
11, 11143–11204, 2011

Table 6. Seasonal comparison statistics between calculated Na^+ air concentrations and observations in 2006, obtained with the EMEP model using M&M, G03, A98, SH98 and V01 source functions. Note: year daily) statistics compare calculated and observed Na^+ concentrations on a daily basis.

	EMEP (M&M)		G03		A98		SH98		V01	
	Bias	*R*	Bias	*R*	Bias	*R*	Bias	*R*	Bias	*R*
Year (daily)	12	0.69	25	0.68	−10	0.53	−40	0.68	121	0.43
Winter	30	0.62	49	0.60	−4	0.56	−27	0.60	124	0.49
Spring	10	0.67	25	0.67	−11	0.56	−40	0.66	114	0.48
Summer	6	0.70	13	0.69	26	0.52	−47	0.69	245	0.44
Autumn	5	0.71	13	0.71	27	0.58	−45	0.69	73	0.49

ACPD
11, 11143–11204, 2011

Table 7. Comparison of Na^+ in air calculated using three meteorological drivers (PARLAM-PS, HIRLAM-v7.1 and ECMWF) with the EMEP observations in 2006.

		PARLAM-PS			HIRLAM-v7.1			ECMWF		
	Obs	Mod	Bias	*R*	Mod	Bias	*R*	Mod	Bias	*R*
Year	0.91	1.02	12	0.69	0.94	4	0.83	0.9	0	0.82
Winter	0.84	1.09	30	0.62	0.95	13	0.66	0.81	−4	0.64
Spring	0.89	0.97	10	0.67	0.98	11	0.66	0.91	2	0.69
Summer	0.64	0.68	6	0.70	0.56	−13	0.75	0.79	23	0.73
Autumn	1.06	1.11	5	0.71	1.07	1	0.72	0.97	−9	0.67

ACPD
11, 11143–11204, 2011

Table 8. Model bias (in %) for concentrations of Na^+ in air and precipitation in sensitivity tests to scavenging ratio W, below-cloud washout efficiency (E), dry deposition reduction and including larger aerosols for 2006.

	$W = 1 \times 10^6$	$W = 1.6 \times 10^6$	$W = 2 \times 10^6$	$E = 1$	0.5 Vd	Size ext.	Size ext. $W = 2 \times 10^6$
Na^+ air	12	5	−2	−1	66	12*	−2*
Na^+ prec	−64	−62	−62	−65	−51	−51	−49

* Sea salt aerosols smaller than approximately 10μm.

ACPD
11, 11143–11204, 2011

Table A1. EMEP sites (http://tarantula.nilu.no/projects/ccc/sitedescriptions/index.html).

Country	Site code	Site name	Lat	Lon
Austria	AT02	Illmitz	47°46′ N	16°46′ E
Germany	DE01	Westerland	54°56′ N	08°19′ E
	DE02	Langenbruegge	52°48′ N	10°45′ E
	DE03	Schauinsland	47°55′ N	07°54′ E
	DE07	Neuglobsow	53°09′ N	13°02′ E
	DE09	Zingst	54°26′ N	12°44′ E
	DE44	Melpitz	51°32′ N	12°56′ E
Denmark	DK03	Tange	56°21′ N	9°36′ E
	DK05	Keldsnor	54°44′ N	10°44′ E
	DK08	Anholt	56°43′ N	11°31′ E
	DK31	Ulborg	56°17′ N	8°26′ E
Finland	FI09	Utö	59°47′ N	21°23′ E
	FI17	Virolahti	60°31′ N	27°41′ E
	FI36	Pallas	68°00′ N	24°15′ E
Ireland	IE01	Valentia Obs.	51°56′ N	10°15′ W
	IE05	Oak Park	52°52′ N	6°55′ W
	IE06	Malin Head	55°23′ N	7°20′ W
	IE08	Carnsore Point	52°11′ N	6°22′ W
Iceland	IS02	Irafoss	64°05′ N	21°01′ W
Norway	NO01	Birkenes	58°23′ N	8°15′ E
	NO15	Tustervatn	65°50′ N	13°55′ E
	NO39	Kaarvatn	62°47′ N	8°53′ E
	NO42	Zeppelin	78°54′ N	11°53′ E
	NO55	Karasjok	69°28′ N	25°13′ E
Slovenia	SI08	Iskrba	45°34′ N	14°52′ E
Slovakia	SK04	Stara Lesna	49°09′ N	20°17′ E
	SK06	Starina	49°03′ N	22°16′ E

ACPD
11, 11143–11204, 2011

Table A2. Model bias and correlation for daily Na^+ concentrations in air for 2006 compared to observations at EMEP sites .

		M&M		G03		A98		SH98		V01	
	Obs	Bias	*R*	Bias	*R*	Bias	*R*	Bias	*R*	Bias	*R*
AT02	0.10	−41	0.03	−41	0.04	−73	0.02	−79	0.04	−10	−0.01
DE01	1.56	0	0.81	18	0.81	−13	0.52	−42	0.81	109	0.34
DE02	0.39	−30	0.64	−25	0.63	−60	0.42	−70	0.63	15	0.34
DE03	0.14	−40	0.53	−42	0.50	−78	0.44	−80	0.49	−27	0.38
DE07	0.37	−41	0.63	−38	0.60	−66	0.38	−76	0.58	1	0.33
DE09	0.57	9	0.74	25	0.73	14	0.38	−42	0.73	200	0.26
DK03	0.97	−26	0.79	−16	0.79	−42	0.51	−62	0.79	50	0.33
DK05	1.10	1	0.72	18	0.71	16	0.29	−43	0.72	198	0.02
DK08	1.52	−1	0.81	16	0.80	26	0.35	−43	0.80	229	−0.12
DK31	1.31	−7	0.83	8	0.83	−24	0.57	−49	0.83	87	0.39
IE01	2.06	64	0.56	91	0.58	30	0.14	−5	0.58	202	−0.09
IE05	1.00	5	0.59	17	0.59	−30	0.19	−47	0.60	76	−0.01
IE06	2.44	17	0.69	38	0.70	−11	0.39	−31	0.71	101	0.13
IE08	3.66	−51	0.65	−44	0.65	−60	0.32	−73	0.66	−1	0.12
IS02	1.00	72	0.56	109	0.57	21	0.24	3	0.57	173	0.09
NO01	0.44	−10	0.64	−1	0.62	−39	0.31	−59	0.60	70	0.21
NO15	0.25	98	0.54	140	0.54	45	0.39	16	0.54	239	0.32
NO39	0.16	109	0.56	151	0.55	46	0.45	21	0.55	240	0.41
NO42	0.25	450	0.40	597	0.41	464	0.05	252	0.41	1282	−0.08
NO55	0.23	37	0.58	67	0.59	−3	0.38	−25	0.59	147	0.29
SI08	0.14	−44	0.4	−46	0.37	−38	0.33	−80	0.37	110	0.3
SK04	0.19	−71	0.08	−70	0.06	−86	0.09	−89	0.04	−54	0.12
Mean	0.90	23	0.58	44	0.58	2	0.33	−32	0.57	156	0.19

ACPD
11, 11143–11204, 2011

Table A3. Statistical analysis of Na^+ air concentrations calculated with the EMEP and the SILAM models against measurements in 2007.

		EMEP				SILAM			
	Obs	Mod	Bias	Corr	RMSE	Mod	Bias	Corr	RMSE
AT02	0.09	0.07	−32	0.54	0.08	0.07	−27	0.60	0.08
DE01	2.54	1.89	−35	0.55	3.06	2.80	10	0.56	2.92
DE02	0.53	0.4	−35	0.57	0.54	0.33	−37	0.72	0.47
DE03	0.17	0.1	−45	0.42	0.25	0.13	−24	0.44	0.26
DE07	0.48	0.3	−46	0.56	0.62	0.28	−41	0.68	0.56
DE09	0.94	0.89	−17	0.67	0.70	0.62	−34	0.82	0.63
DK03	1.28	0.94	−36	0.58	1.20	0.99	−23	0.54	1.18
DK05	1.35	1.78	16	0.8	0.86	1.36	1	0.72	0.73
DK08	1.92	2.03	−8	0.82	0.86	2.09	9	0.73	1.06
DK31	1.71	1.58	−19	0.82	0.88	1.68	−2	0.83	0.85
FI09	0.38	2.59	498	0.74	2.38	0.50	31	0.62	0.33
FI17	0.2	0.51	128	0.73	0.41	0.11	−45	0.58	0.17
FI36	0.17	0.14	−30	0.43	0.22	0.13	−24	0.44	0.21
IE01	2.47	3.07	9	0.68	1.92	2.31	−7	0.69	1.91
IE05	0.89	0.89	−12	0.54	0.69	0.68	−24	0.66	0.60
IE06	2.43	3.13	13	0.65	1.73	1.91	−22	0.68	1.55
IE08	3.51	1.51	−63	0.79	3.25	1.36	−61	0.77	3.27
IS02	0.95	1.28	18	0.54	1.07				
NO01	0.35	0.32	−21	0.59	0.39	0.51	45	0.73	0.38
NO15	0.29	0.59	74	0.45	0.62	0.54	85	0.63	0.51
NO39	0.17	0.49	158	0.41	0.58	0.33	94	0.37	0.39
NO42	0.23	0.59	123	0.31	0.64				
NO55	0.22	0.25	0	0.47	0.28	0.28	26	0.56	0.30
SI08	0.11	0.08	−39	0.47	0.15	0.09	−21	0.75	0.11
SK04	0.09	0.05	−49	0.52	0.08	0.06	−29	0.42	0.11
SK06	0.08	0.07	−20	0.53	0.08	0.07	−16	0.50	0.10

ACPD
11, 11143–11204, 2011

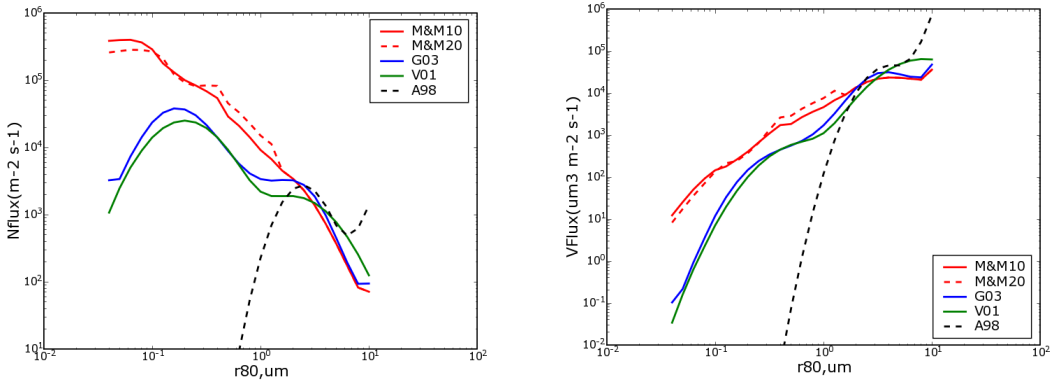

Fig. 1. Sea spray number (left) and volume (right) flux as a function of droplet radius at 80% relative humidity, calculated with the M&M, V01, G03 and A98 source functions for the wind speed 10 m s^{-1}. M&M10 and M&M20 are fluxes calculated at the sea temperature of 10 °C and 20 °C.

ACPD
11, 11143–11204, 2011

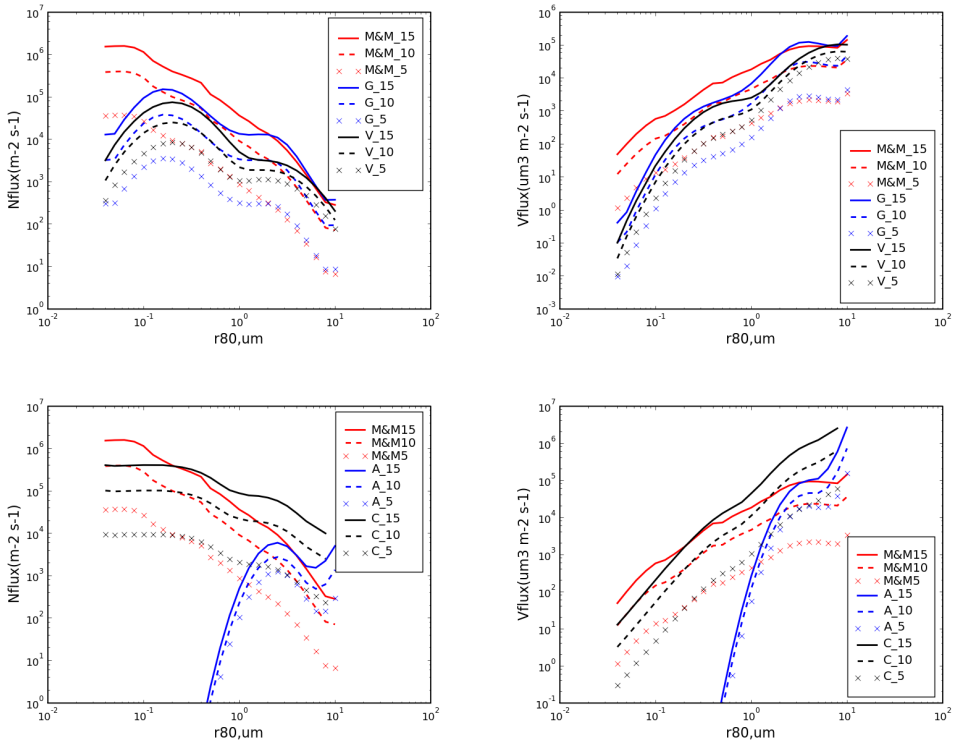

Fig. 2. Sea spray flux as a function of droplet radius at 80% relative humidity calculated with the M&M source functions are compared to those from V01 and G03 (upper panel), A98 and C06 (lower panel) for wind speeds of 5, 10 and 15 m s^{-1}: sea spray number (left) and volume (right).

ACPD
11, 11143–11204, 2011

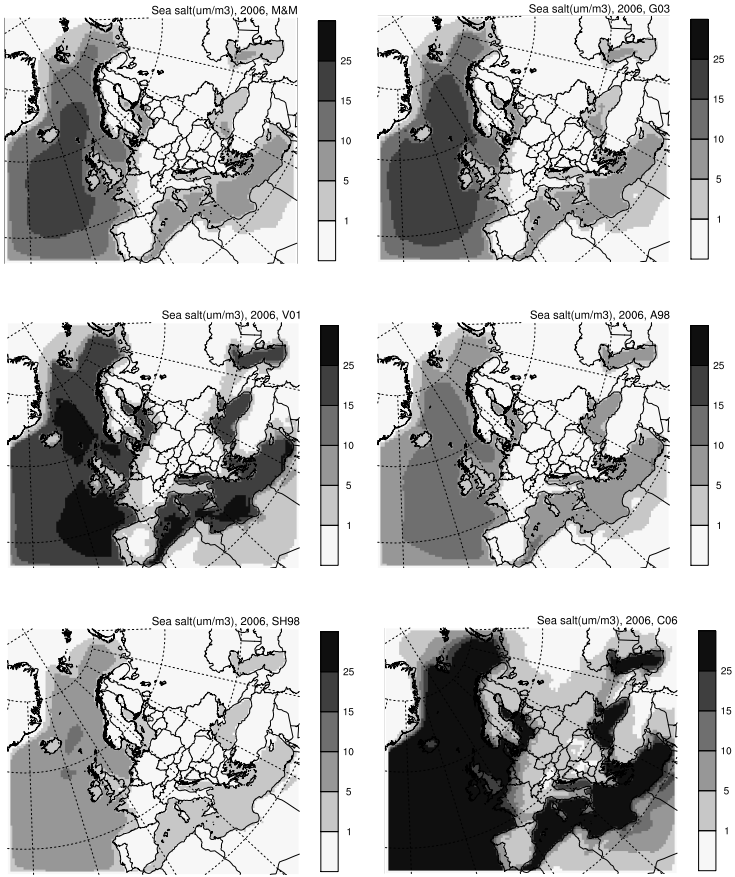

Fig. 3. Annual mean concentrations of sea salt in 2006 calculated with the standard EMEP model, i.e. using M&M source function (upper left), and using source functions of G03 (upper right), V01 and A98 (middle row), and of SH98 and C06 (lower row).

ACPD
11, 11143–11204, 2011

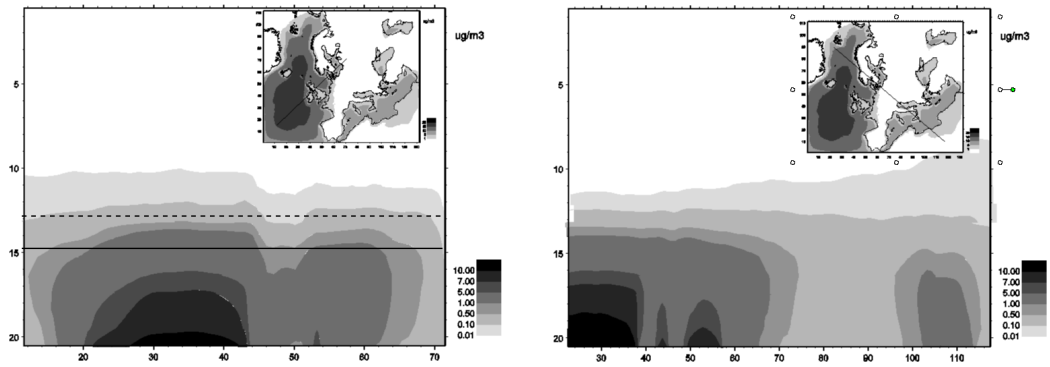

Fig. 4. Vertical cross-sections of annual mean sea salt concentration in 2006. The abscissa corresponds to the EMEP x-axes, while the ordinate axes show the centres of model vertical layers. The solid and dashed lines mark approximately 1 and 2 km heights, respectively.

ACPD
11, 11143–11204, 2011

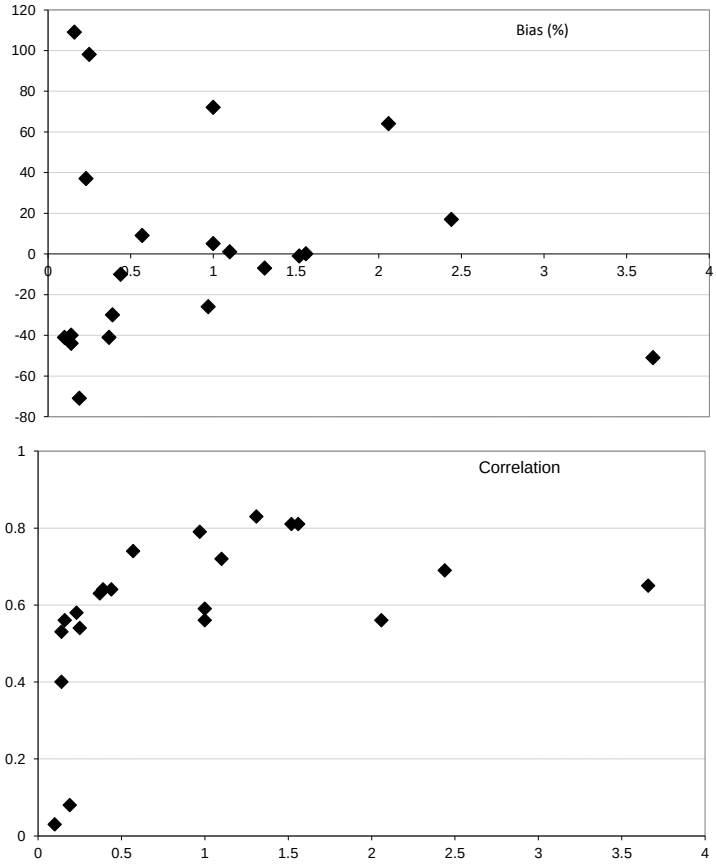

Fig. 5. Bias (%) **(a)** and correlation **(b)** for calculated versus measured Na^+ in air in 2006 for EMEP sites ranked from left to right according to increasing measured Na^+ concentrations (given in $\mu g\, m^{-3}$ on the abscissa axis).

ACPD
11, 11143–11204, 2011

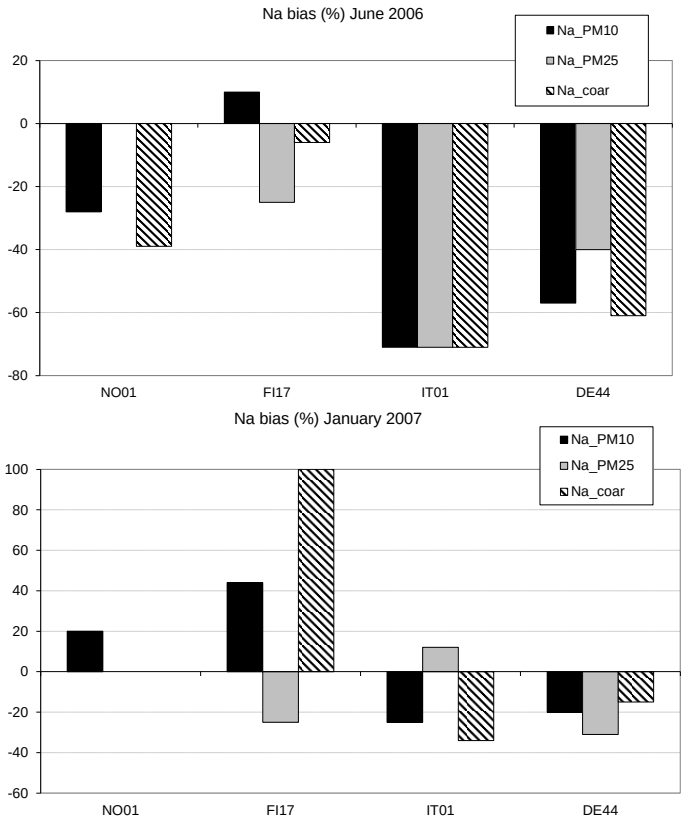

Fig. 6. Model bias for concentrations Na^+ in PM_{10}, Na^+ in $PM_{2.5}$ (fine Na^+) and coarse Na^+ at Birkenes (NO01), Virolahti (FI17), Montelibretti (IT01) and Melpitz (DE44) in June 2006 (left) and January 2007 (right). Note: (1) the bias for Na_$PM_{2.5}$ is zero for NO01 in June 2006; (2) suspected erroneous data in January 2007 was excluded for NO01; (3) less days with measurements for Na_$PM_{2.5}$ and Na_coar than for Na_PM_{10} at FI17.

ACPD
11, 11143–11204, 2011

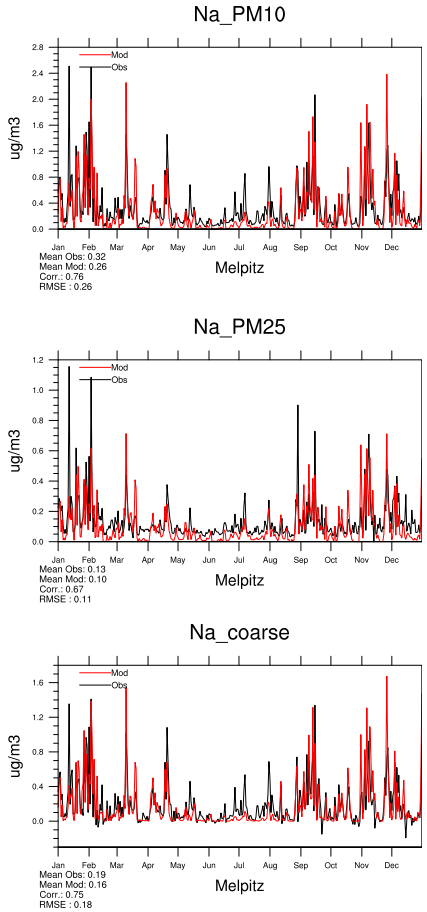

Fig. 7. Daily time-series of observed and model calculated air concentrations of Na^+ PM_{10}, $PM_{2.5}$ and coarse PM in 2007 at Melpitz, Germany (DE44).

ACPD
11, 11143–11204, 2011

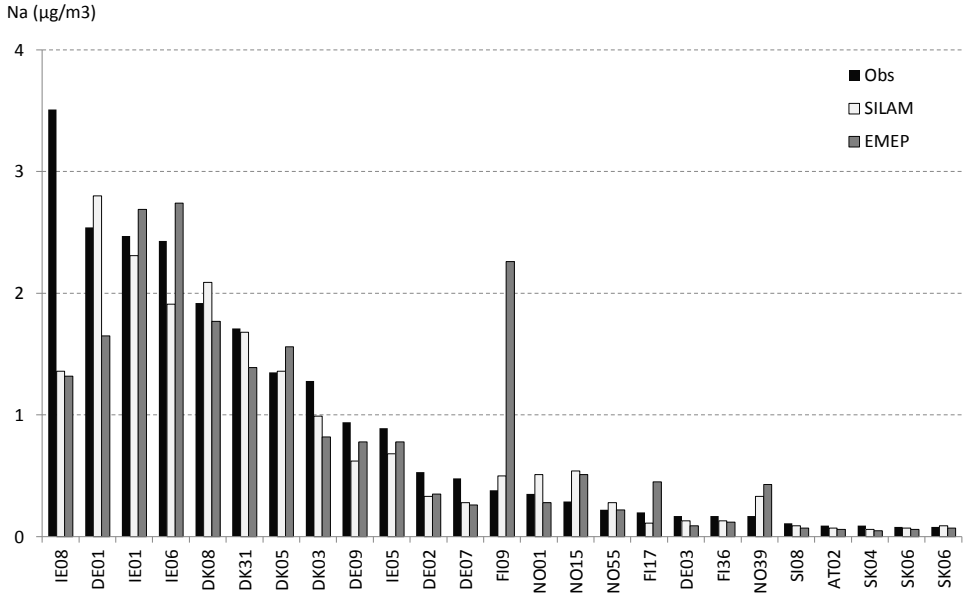

Fig. 8. Annual mean Na^+ air concentrations at EMEP sites in 2007: observed (black) and from the SILAM (white) and the EMEP (grey) models with observed values. The sites are ranked according to decreasing measured concentrations.

ACPD
11, 11143–11204, 2011

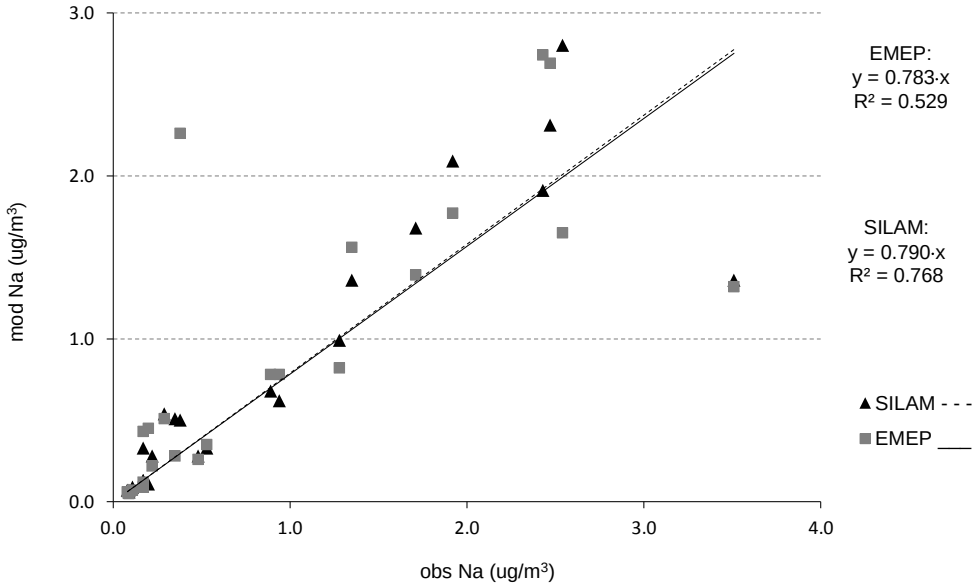

Fig. 9. Scatter-plots for Na^+ air concentrations calculated with the SILAM (triangles) and the EMEP (squares) model versus observed values at EMEP sites in 2007.

ACPD
11, 11143–11204, 2011